Pulsed laser deposition of boron and boron nitride thin film

A Thesis Presented for the

Master of Science

Degree

The University of Tennessee, Knoxville

Siwei tang

August 2011

DEDICATION

To my wife Tian and my parents

ACKNOWLEDGEMENT

Firstly, I would like to thank Dr. Philip D. Rack who is my advisor, mentor and friend over the past two years. He is always guidance and an example that encouraged me. Secondly, I would like to thank my friends in our group: Carlos Gonzales, Yueying Wu, Jiyong Noh, Joohyon Noh, Daryl Smith, John Peak and etc. Thanks for their help with everything. Thirdly, I would like to thank my wife Tian Tang, who is always encouraging me and let me be confidence when I am down.

ABSTRACT

This thesis focuses on the preparation parameter and characterization of boron and boron nitride thin film. System is built composing of designing the geometry, substrate and target holder, pumping parts and plasma generated parts. Experiments with various conditions have been tried and the optimized condition is found for the film growth rate. Many ways of characterization includes: X-ray diffraction, Scanning electron microscopy, Raman spectroscopy, Fourier transform infrared spectroscopy have been tried to identify the material composition.

TABLE OF CONTENTS

ACKNOWLEGEMENT……iii

ABSTRACT……...iv

TABLE OF CONTENSTS……...…….……..v

CHAPTER I INTRODUCTION……1

1.1 Project motivation…….....1

1.2 Boron and boron compounds……..2

1.3 Pulsed laser deposition……....2

Reference .....……..4

CHAPTER II LITERATURE REVIEW…….……5

2.1 Basic laser physics……..5

2.2 Laser-solid interaction……6

2.2.1 Material optical properties……6

2.2.2 Absorption mechanism…….7

2.3 Thin film growth……....9

2.4 Boron and boron nitride prepared by pulsed laser deposition……..12

2.5 Theory of neutron capture…….19

Reference……...……...21

CHAPTER III EXPERIMENT SETUP……..……..22

3.1 Pulsed laser system set up…….22

3.1.1 Laser system……22

3.1.2 Target……..22

3.1.3 Deposition chamber……22

3.1.4 Optical parts……24

3.1.5 Substrate holder and target holder……..24

3.1.6 Plasma generation part……24

3.2 Experiment processing……..28

3.2.1 Working pressure……28

3.2.2 Energy density measurement vs. focus length……28

3.2.3 Energy density vs. Plume shape……..31

3.3 Characterization techniques……..33

3.3.1 Filmetrics thin film analyzer……...33

3.3.2 Grazing angle incident beam X-ray diffraction……..33

3.3.3 Scanning electron microscopy……34

3.3.4 Energy-dispersive X-ray spectroscopy……...34

Reference…….....36

CHAPTER IV CHARACTERIZATION…….……37

4.1 Energy density influence……..37

4.1.1 Plume profile and thickness profile……37

4.1.2 Samples prepared under different fluence…….40

4.2 Substrate-target distance influence……...50

4.3 Annealing study……60

4.4 Reactive pulsed laser deposition……...64

Reference……..84

CHAPTER V CONCLUSION……..……85

VITA……..86

LIST OF TABLES

Table Page

Table 4.1. Energy density vs. thickness (tilting with vertical direction)……..…….42

Table 4.2. Energy density vs. thickness (tilting with horizontal direction) ….…….……46

Table 4.3. Energy density vs. thickness (tilting with horizontal direction) after change target and refill the gas…….……...47

Table 4.4. Distance vs thickness……51

Table 4.5. Samples prepared under 3 min (1200 pulses) at 666 mJ/cm^2……..….65

Table 4.6. Samples prepared under 30 min (9000 pulses) at 582 mJ/cm^2…….67

LIST OF FIGURES

Figure 2.1. Laser interactions with material……8

Figure 2.2. Diagram of different thin film growth mode: above left is island growth mode; bottom right is layer growth mode; bottom left is island-layer growth mode……...……11

Figure 2.3. Laser energy dependence on the surface morphology of boron film deposited at 900°C, 50 Pa by laser ablation……...14

Figure 2.4. Laser energy dependence on the XRD spectra of boron films deposited at 900°C, 50 Pa by laser ablation……15

Figure 2.5. X-ray diffractograms of boron nitride samples deposited at different temperatures in the 2u CuK_{α} region……16

Figure 2.6. (a) Microstructure of BN thin film prepared without Nitrogen plasma (b) Microstructure of BN prepared with Nitrogen plasma……..17

Figure 2.7. XRD spectrum of boron nitride deposited at 473K on silicon (100) with RF nitrogen plasma (a) and without (b)…….18

Figure 3.1. Beam Profile obtained from Lambda Physik LPX 300 Laser…….23

Figure 3.2. Basic design of the pulsed laser deposition system (a) and system construction (b) target and substrate-target relative positions (c)……26

Figure 3.3. (a) The plasma-generated part (b) Principle for plasma generating (c) Voltage of plasma generation vs. nitrogen pressure……27

Figure 3.4. The substrate holder with adjustable holes which are 1 cm from each other……..29

Figure 3.5. (a) Spot area vs. distance from target to lens (b) Energy density vs. distance from target to lens……...30

Figure 3.6. Plume shape vs. energy density……...32

Figure 3.7. (a) Filmetrics thin film analyzer system F20 (b) X-ray diffraction equipment and optical parts set up (c) Principle of SEM……...35

Figure 4.1. $Cos^{n}\theta$ vs. θ and the shape of plume in the polar figure……..……38

Figure 4.2. (a) The image of the sample prepared by PLD (b) the thickness distribution on the sample……39

Figure 4.3. Two geometrical ways of target-substrate locations……...40

Figure 4.4. SEM images of boron thin film typical morphology prepared with along with the vertical direction……44

Figure 4.5. SEM images of boron thin film typical morphology prepared with horizontal direction…….49

Figure 4.6. (a) thickness of the thin film middle point vs. target- substrate distance (b) the thickness distribution of samples surface vs. distance from middle point of the sample……..53

Figure 4.7. Thickness vs. distance curve with exponential function fit……..54

Figure 4.8. SEM images of samples prepared with various target-substrate distances…….55

Figure 4.9. Cross-section SEMs comparing with samples prepared under different target-substrate distances……..57

Figure 4.10. (a)Surface look of the sample annealed after 1200°C (b) The boron peaks existed in the sample annealed after 1200°C…….61

Figure 4.11. Comparing of GIXRD pattern of sample (a) annealing at 1200°C, 1000°C and without annealing for one hour (b) annealing at 1100°C, 1000°C, 900°C and 800°C for two hours……...62

Figure 4.12. SEM images of boron thin film sample after 1200°C annealing for one hour……..63

Figure 4.13. Pressure vs. thickness in different conditions……68

Figure 4.14. Mean free path vs. pressure……...69

Figure 4.15. SEM images of samples prepare under different pressure……71

Figure 4.16. SEM images of samples prepare(900 pulses) under different pressure……74

Figure 4.17. (a) XRD patterns of samples prepared in 1200 pulses (b) XRD patterns of samples prepared in 9000 pulses…….77

Figure 4.18. (a) Raman spectra of boron nitride and boron prepared under different conditions (b) Raman spectra of boron nitride prepared under different temperature……..78

Figure 4.19 FTIR spectra of samples: (a) samples prepared under 1200 pulses (b) samples prepared under 9000 pulses (c) FTIR spectra in literature……79

Chapter 1 Introduction

1.1 Project motivation

The main goal of our recently funded program is to explore the possibility of "pulsed laser deposition of boron phosphide (BP) as thermal neutron detector". The research thrust is divided into three ways: 1), thin film growth parameters are investigated to find the best for high-quality boron phosphide growth; 2), characterize boron phosphide thin film samples prepared in different parameters and figure out the best performance. Third, devices design for thermal neutron detector.

As a result, it is very important to understand and be familiar with the pulsed laser deposition process (especially the controlling parameters: pressure, energy density, laser wavelength, repetition rate, etc.), boron related compounds, and finally principle of neutron device operation (theory and performance test).

As will be demonstrated, preliminary BP pulsed laser deposition (PLD) was attempted from a pressed and sintered target, but quickly abandoned for a reactive approach. To this end, this thesis focused on the investigation of effect of various energy densities on boron thin films prepared by pulsed laser deposition.

In previous experiments, the boron and boron compounds are prepared through chemical vapor deposition with reaction of B_2H_6 and PH_3. However, there are few PVD (physical vapor deposition) experiments involving boron and boron compounds. So, one major purpose of our

experiment is to compare and understand the differences between samples prepared by both CVD and PVD process and determine the optimized conditions.

1.2 Boron and boron compounds

Boron is a kind of metalloid which has properties between metal and non-metals. It is a brown powder in amorphous structure and black in crystalline. It is used for doping as an acceptor in silicon semiconductor devices. Boron is hard and has a high melting point about 2076°C. Boron has rhombohedral, orthorhombic, tetragonal structure and it has a band gap of 1.6-2.1 eV[1].

Boron nitride (BN) is a kind of III-V semiconductor material; it is the second hardest material known to man. BN has excellent thermal and chemical stability. It shares the same phase as carbon: carbon has hexagonal graphite which is most stable and cubic diamond phase which is the hardest of all materials; boron nitride has hexagonal phase which is also most stable and cubic phase which is hardest among its phases.[3]

1.3 Pulsed laser deposition

Pulsed laser deposition shares several similarities with physical vapor deposition. They do not involve chemical reactions per se and the main processes of them are physical phase transformations of the target material and deposited on substrate without changing chemical structure.[3] However, reactive PVD process is incorporate a reactive gas (Oxygen, Nitrogen…) and react with the physically deposited material during synthesis. Pulsed laser deposition includes three steps: heating and ablation of material, transmission of material through a medium,

and condensation of the material when it reaches substrate for growth. [4] So the process are highly dependent on the laser energy density, duration time, repetition rate, wavelength and target material optical properties(absorption, reflectance, transmittance) and thermal properties(thermal conductance, thermal diffusivity, melting point and etc.).

There are many merits of pulsed laser deposition: firstly, stoichiometric transfer of material especially many kinds of super-conductive material (metallic oxide) can be achieved. The composition of thin film can be controlled by process parameters and closely resemble the target material. Secondly, higher deposition rate can be fulfilled because energy density is able to be high enough for melting and vaporizing surface of target. Thirdly, laser source is out of the experiment chamber so that adding background gas or vacuum will not influence the behavior of laser source.[3]

However, there are also many disadvantages existed. Particles generation and non uniform distributions of thin film thickness are two main problems. These kinds of problems are attributed to the nature of pulse laser deposition: the condensation of vapor and shape of plume. Researchers are trying many methods such as rotating target, adding a particle filter and etc to avoid them.

References

1. http://en.wikipedia.org/wiki/Boron

2. http://en.wikipedia.org/wiki/Boron_nitride

3. Robert Eason , Pulsed Laser Deposition of Thin Films, Wiley, New York, 2007.

4. D.B. Chrisey and G.K. Hubler, Eds., Pulsed Laser Deposition of Thin Films, Wiley, New York, 1994.

Chapter 2 Literature Review

2.1. Basic laser physics

Laser is coming from a combination of simple words which describe its basic principle: "light amplification by stimulated emission of radiation".[1] To begin with explaining the physical mechanism of laser, it is necessary to know the concept named population inversion. This phenomenon is referring atoms absorbing energy and resulting in many of its electrons in higher energy state. Population inversion is called in the case that there are more electrons in higher energy state than that in lower energy state. In the meantime, if light is passing through, the high energy electrons are stimulated and able to fall into the lower energy state which will emit photons. So the total energy of output photon is larger than the input photons. As a result, the laser beam is emerged.

There is no limit for the stimulated medium. It could be any kinds of phase: gas, liquid, solid and even plasma. In our lab, 248 nm KrF eximer a gas laser system is used. The reason for using gas laser is due to many advantages of gas. The changeable shape of gas demands low requirement of medium container; the vacuum technology will increase the purity of gas and recycle it which can increase the life time; the flow rate of gas is relative fast and easily used for heat conducting; also the gas laser wavelength can be ranging from far infrared to x-ray[2].

Especially, KrF eximer gas laser uses a krypton-neon buffer gas and fluorine to produce laser irradiation. The neon buffer gas plays an active role in the process, while krypton and fluorine are ionized by the energy transferred into the system. These electrons and ions combines together to form ion-pair excited state as follows[3]:

$$Kr^+ + F^- + Kr \rightarrow (Kr^+F^-)^* + Kr \qquad 2.1$$

When there is light coming in, the excited ion-pair de-excites to its ground state and dissociates into krypton and fluorine atoms. Energy emitted in this process will be transferred into output photons.

$$Photon\ energy + (Kr^+F^-)^* \rightarrow Kr + F + larger\ photon\ energy \qquad 2.2$$

2.2 Laser-solid interaction

2.2.1 Material optical properties

Optical properties have much strong effect on the laser-solid interaction when laser is used to process material. As a specific type of light, lasers also can be reflected, transmitted, absorbed by the irradiated material, the extent of each are largely depending on the reflectance in and absorption coefficient. The reflectance R is given to measure how much in percentage the light will be reflected and absorption coefficient α of unit of cm^{-1} is used to measure the absorption ability of a material. It is expressed by Beer-Lambert law in formula 2.3.

$$I = I_0 e^{-\alpha z} \qquad 2.3$$

Which I is the intensity of light in depth of z distance, I_0 is the intensity of light irradiated on the surface of material in depth z=0.

$$\Phi(z)=I_0(1-R)\alpha e^{-\alpha z} \qquad 2.4$$

Considering the reflectance, formula 2.4 is uses to calculate the light intensity I at a distance z from irradiated surface[3].

However, the refractive index is also able to be used to characterize the optical properties of material. The complex refractive index **n** can be expressed in 2.5 below:

$$\mathbf{n}=n+ik \tag{2.5}$$

Where n is real part of refractive index and k is extinction or absorption index which is related to absorption coefficient in formula 2.6.Both of them can be used to calculate the reflectance in formula 2.7.

$$\alpha=4\pi k/\lambda \tag{2.6}$$

$$R=\frac{(n-1)^2+K^2}{(n+1)^2+K^2} \tag{2.7}$$

2.2.2 Absorption mechanism

The absorption mechanism is mainly dependent on how much energy the photon carries compared to the band-gap energy. Insulators are materials of large band gap and metal is material of near-zero band gap. It is convenient to explain them by considering that they are all semiconductors with various band gaps.

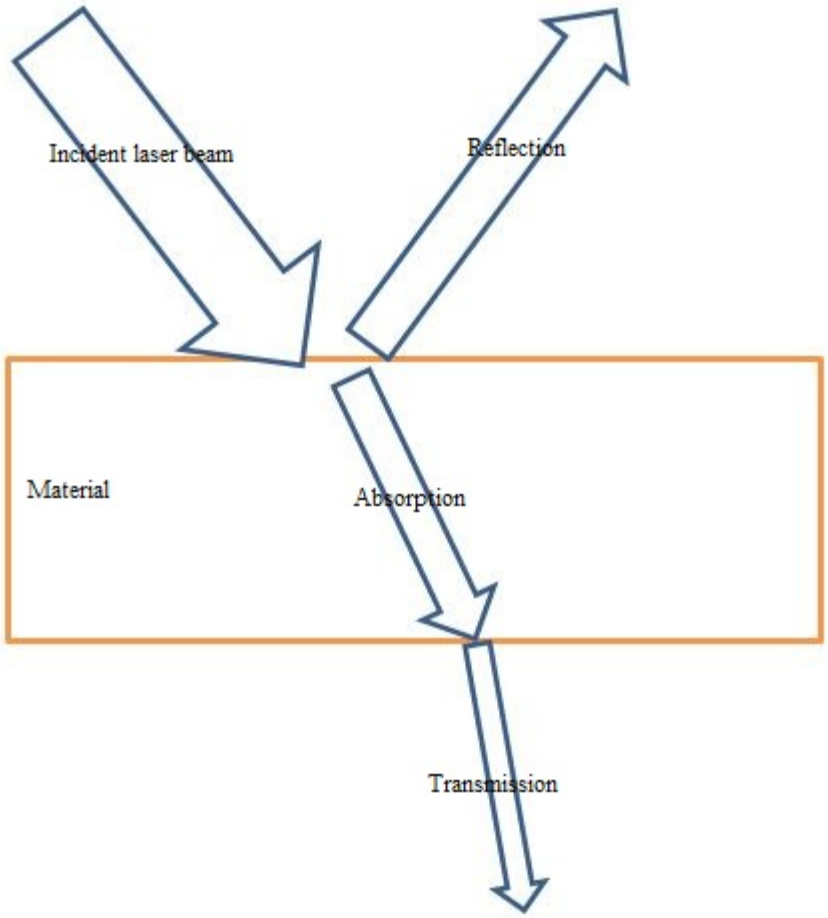


Figure 2.1. Laser interactions with material

Therefore in different energy conditions, absorption mechanisms of laser in semiconductors are divided into three kinds[4] without neglecting doping effects:

[1] If energy carried by photons is smaller compared to the band-gap energy (E_g), the material lattice could be excited directly and result in vibrations. The absorption process is dominated by this kind of effect especially when the lattice vibration is corresponding to wavelength of the laser.

[2] If the photon energy increases and is larger than the band-gap energy E_g, inter band absorption will happen. The main part of this absorption will lie on the direct and indirect excitation of electron-hole pairs assisted by phonon. First, energy will be transferred to electrons of negative charge so that it is able to jump from the valence band to conduction band, leaving holes of positive charge in the valence band. After that, a pair of hole-electron exists. In direct excitation, the electron moves to conduction band with same wave vector, however, in indirect excitation, the electron will move to conduction band with different wave vector. If the energy density keeps increasing, electron-hole plasma is able to appear which absorbs laser beam strongly.[3]

[3] When photon energy increases and is much larger than the band-gap energy E_g. The crystalline lattice symmetry can be broken and surface of the material can become amorphous.

2.3 Thin film growth

The main process of a thin film growth is composed of three parameters: first, there must be the source of material which generates atoms, molecular, particles droplets or any forms. In sputtering or physical vapor deposition, the main source is a solid target while in chemical vapor deposition it is reactive gas. Second, these forms of materials need to be carried to the surface of substrate, so they are driven by a force to travel in a medium like vacuum and then reach the surface of a sample. Third, material arriving at surface of substrate will deposit on the sample and accumulate with other species and propagate film growth.

In the last step, thin film growth is investigated by many people. But there are only three common accepted growth modes. They are all taken place for decreasing the free energy. The free energy is balanced by substrate surface free energy, material surface free energy and substrate-material interface free energy.

The first growth mode is island growth, also named as Volmer-Weber mode. This happens when atoms or molecular of material surface free energy exceeds substrate-material interface free energy. Therefore material accumulating into three dimensional islands will decrease more energy resulting in a more stable state. The second growth mode is layer growth, also named as Frank-Van Der Merwe mode. Conversely, this mode occurs when material will be more likely to attach to the substrate to form two dimensional layer when the substrate-material interface free energy exceeds material surface free energy. The third growth mode is layer-island mixing growth mode, also named as Stranski-Krastanov mode. In this mode, the layer will grow at the beginning and then on top of the layer island will grow. If substrate and material have a lattice mismatch which resulting in a larger binding energy, the layer mode will dominate, however,

after depositing a layer, the substrate become this layer which will change the substrate-material interface free energy. The island will grow when the "new" substrate-material interface free energy is less than material surface free energy.[5]These modes are shown in Fig 3.2.

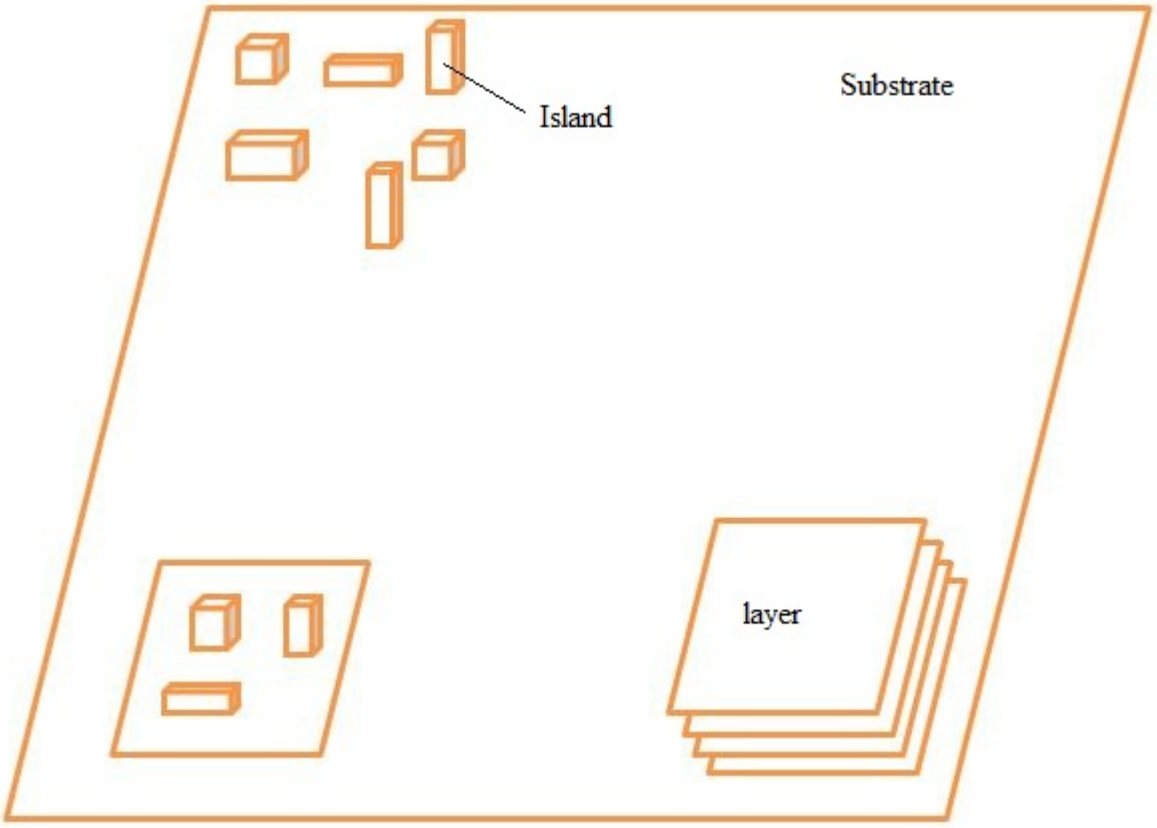


Figure 2.2. Diagram of different thin film growth mode: above left is island growth mode; bottom right is layer growth mode; bottom left is island-layer growth mode

2.4 Boron and boron nitride prepared by pulsed laser deposition

There are not many people who have investigated pulse laser deposition of boron thin films. However, boron and boron compounds are often prepared via chemical vapor deposition. In PLD, traditional PLD is not preferred and researchers often use nitrogen plasma assisted reactive pulsed laser deposition to prepare boron nitride.

Wang [6]prepared boron thin films by pulsed laser deposition exhibiting behavior that there are many spherical particles appearing in lower fluence (50 mJ), however, in higher fluence (250 mJ), the number of particles decreases and accumulate to larger clusters. SEM images are shown in Fig 2.3. XRD shows that in the same substrate temperature (900°C) , samples prepared under higher fluence have more obvious peaks in (110), (104), (021) comparing to that prepared under relative low fluence. That suggests that to some extent increasing fluence will lead to crystallization of boron with substrate temperature around 900°C. XRD patterns are shown in Fig 2.4.

Boron nitride has many crystal forms, the most stable of which is hexagonal boron nitride (h-BN) and cubic boron nitride (c-BN) is less stable. Mitu[7] prepared boron nitride thin films at different substrate temperature and both h-BN and c-BN exist. He found that intensity of h-BN peak decreases and intensity of c-BN peak increase with temperature rising from 400 K-1000K.The evidence is comparing intensity of (002) peak in h-BN and (111) peak in c-BN shown in Fig2.5. It seems amorphous boron nitride prefer to crystallize in cubic form in high temperature. Also, Marotta[8] found that boron reacts with nitrogen plasma more efficient than with nitrogen gas. The SEM images shows without nitrogen plasma boron thin film is likely to

be large clusters and it becomes more even distributed of spherical particles with nitrogen plasma. XRD data in Fig 2.7 shows intensity of plasma-enhanced PLD prepared h-BN (002) peak is about 10 times larger than the same peak without plasma. Comparing to the silicon peak, h-BN is more productive in nitrogen plasma. The plasma can be generated by many ways including RF discharge, DC-bias discharge, and ion beam assisted, field ionization and etc.

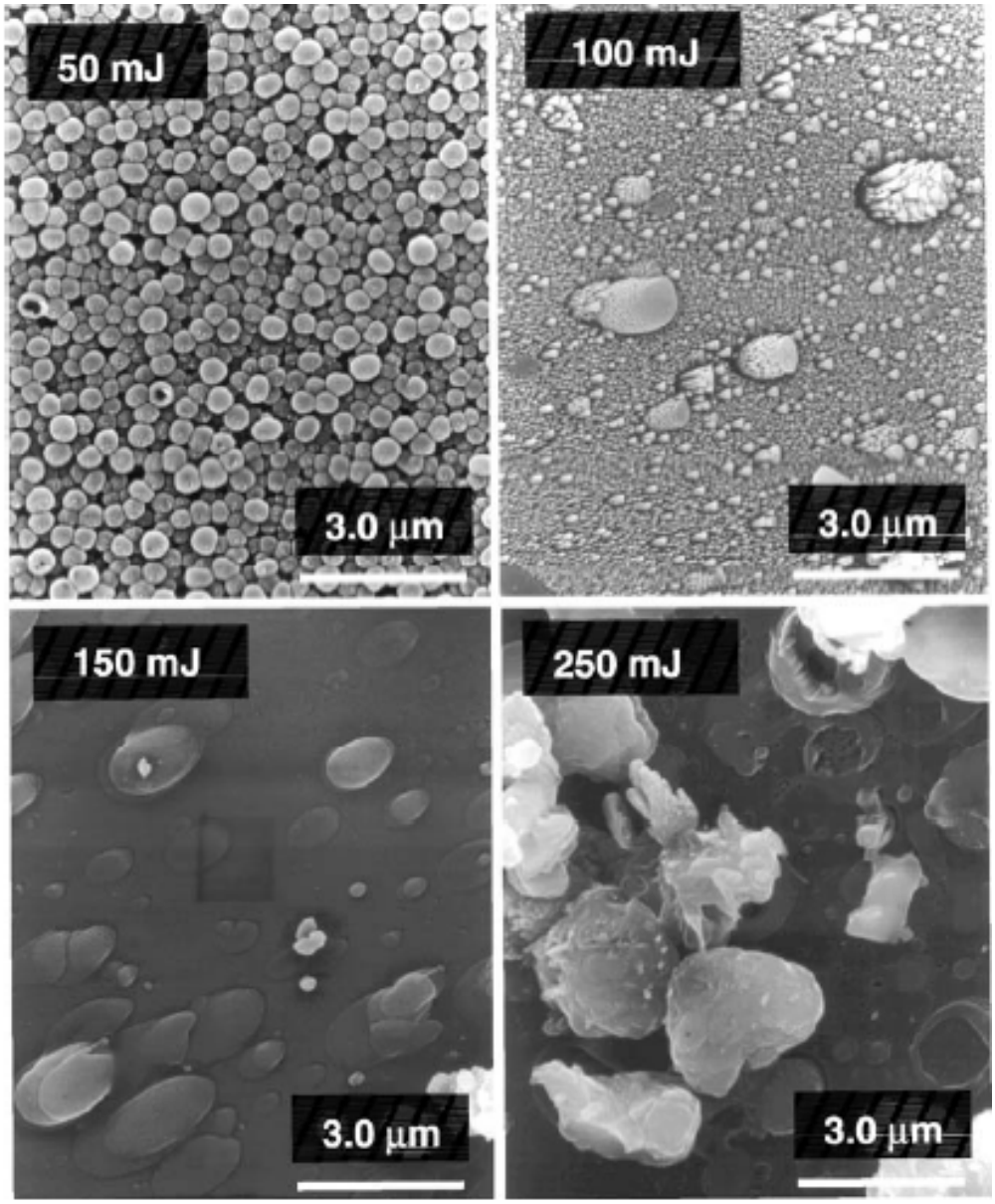


Fig 2.3. Laser energy dependence on the surface morphology of boron film deposited at 900°C, 50 Pa by laser ablation

Source: 6.Zhongke Wang,a Yoshiki Shimizu,an etc. Journal of Solid State Chemistry. 177. 1639–1645.2004

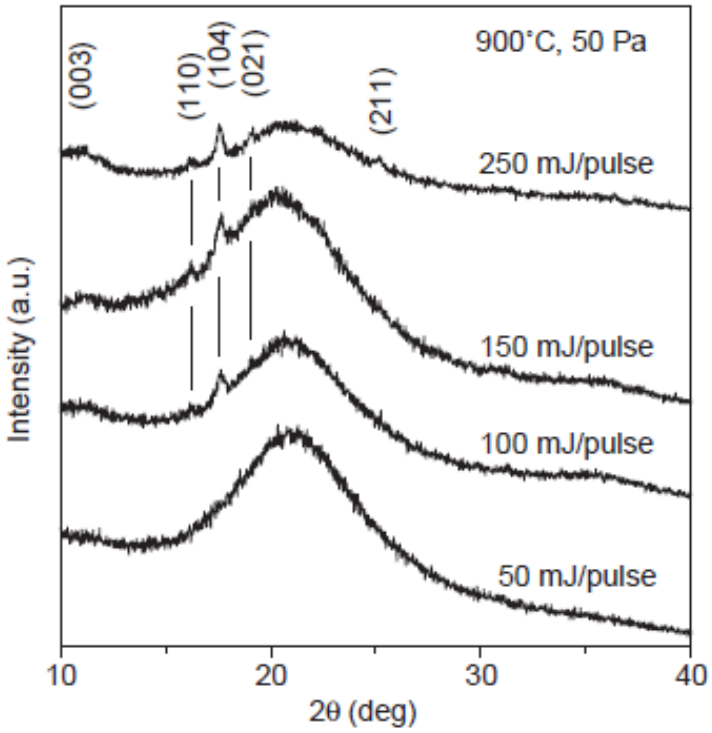


Fig 2.4. Laser energy dependence on the XRD spectra of boron films deposited at 900°C, 50 Pa by laser ablation

Source: 6.Zhongke Wang,a Yoshiki Shimizu,an etc. Journal of Solid State Chemistry. 177. 1639–1645.2004

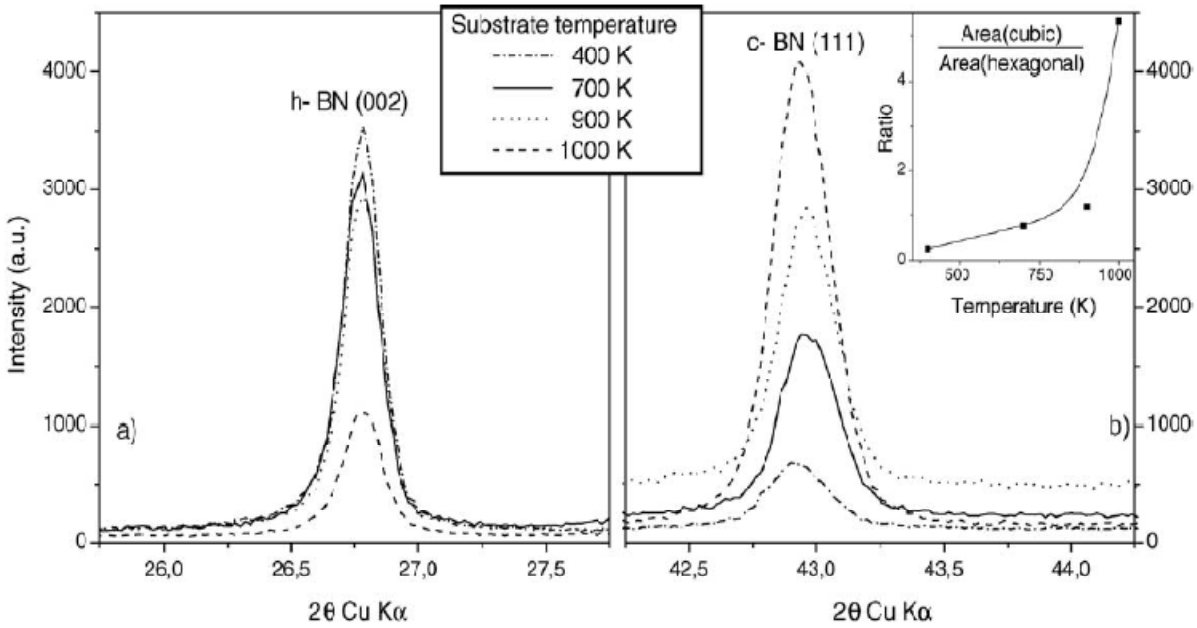
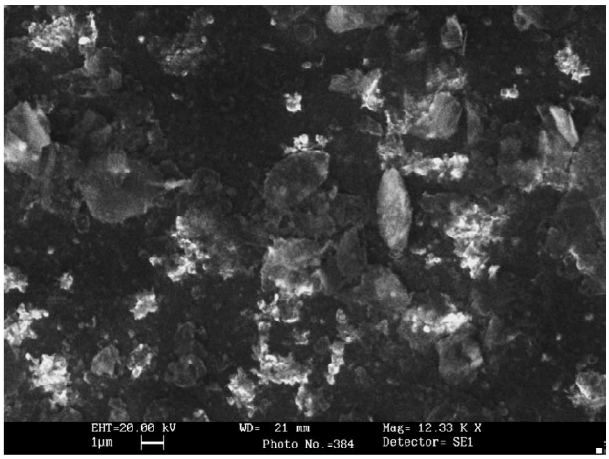
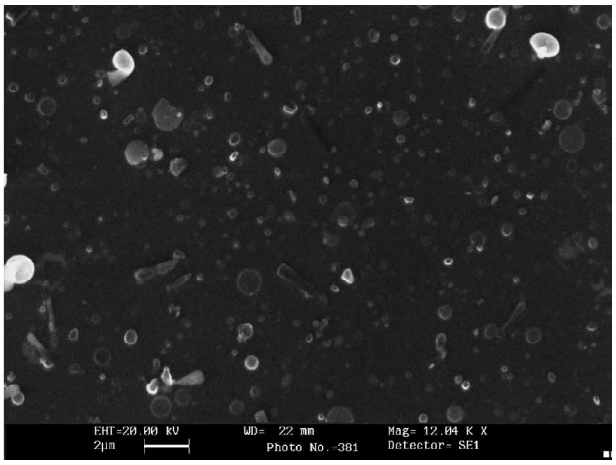


Figure 2.5 X-ray diffractograms of boron nitride samples deposited at different temperatures in the 2u CuK$_\alpha$ region corresponding to (a) (0 0 2) hexagonal-BN; (b) (1 1 1) cubic-BN. In the inset, the ratio of the cubic/hexagonal areas vs. substrate temperature is reported.

Source: 7. B. Mitu, P. Bilkova, V. Marotta, S. Orlando, A. Santagata. 123–127.Applied Surface Science 247 (2005)



(a)



(b)

Figure 2.6.(a) Microstructure of BN thin film prepared without Nitrogen plasma (b) Microstructure of BN prepared with Nitrogen plasma

Source: 8. V.Marotta, S.Orlando, G.P. Parisi, A.Santagata. Applied Surface Science .575-581. 208-209. (2003)

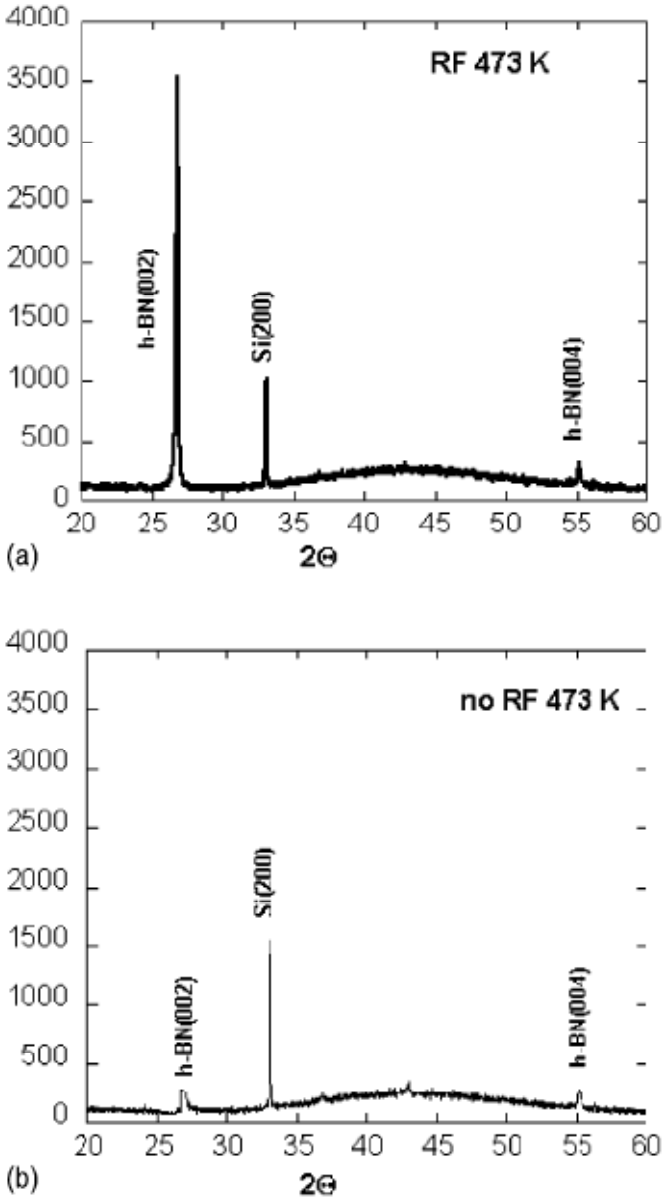


Figure 2.7 XRD spectrum of boron nitride deposited at 473K on silicon (100) with RF nitrogen plasma (a) and without (b)

Source: 8. V.Marotta, S.Orlando, G.P. Parisi, A.Santagata. Applied Surface Science .575-581. 208-209. (2003)

2.5 Theory of neutron capture

Boron, especially ^{10}B, reacts with neutrons easily for equations below:

$$^{10}B + n \rightarrow {}^{7}Li + \alpha + 2.3\ MeV \qquad 2.17$$

Boron element (^{10}B) is one candidate material reacting with thermal neutron due to its large cross section of 3840 barns. This effective cross section represents the absorption ability of material to thermal neutron. After reacting, it is divided into an alpha particle (1.47 MeV) and Lithium (^{7}Li) (0.84 MeV) and emits amount of energy (2.3 MeV). The charged particles which enter the semiconductor material will create electrons and holes.

In real situation, there exists a problem. The thickness of boron layer will have an optimized value because if it is too thick, charged particles are not able to get to the semiconductor material due to limited distance of travelling. However, if the boron layer is too thin, it becomes less efficient to produce hole and electrons.

Boron with an isotopic mass of 10 (^{10}B) is frequently used as a converter material its excellent microscopic thermal neutron absorption cross section of 3840 barns. However, these devices are limited in efficiency due to the conflicting requirements of the ^{10}B neutron converter material. The thermal neutron ^{10}B reaction which populates mostly to the first excited state of ^{7}Li, produces an alpha particle (1.47 MeV) and ^{7}Li (0.84 MeV)[12]. These charged particles subsequently enter the semiconductor detector to create electrons and holes for generation of the electrical signal. However, these particles can travel inside the converter material only for a short

distance (3.3 μm). Thus, if the boron layer is too thick, the charged particles will be absorbed before they reach the semiconductor material.

Reference

1.http://en.wikipedia.org/wiki/Laser

2.Masamori Endo, Robert F. Walter, p.2 in Gas laser, CRC Press, Boca Raton, FL,2006

3.James Brannon, p.7-p.25 in Excimer laser ablation and etching, AVS Press, New York, 1993.

4. R.F.Wood, C.W. White, and R.T Young, p175 in Pulsed Laser Processing of Seminconductors, Academic Press, Orlando, 1984

5. Milton Ohring, p.358 in Materials Science of Thin Films, Academic Press, Singapore, 2006

6. Zhongke Wang,a Yoshiki Shimizu,an etc. Journal of Solid State Chemistry. 177. 1639–1645.2004

7. B. Mitu, P. Bilkova, V. Marotta, S. Orlando, A. Santagata. 123- 127.Applied Surface Science 247 (2005)

8. V.Marotta, S.Orlando, G.P. Parisi, A.Santagata. Applied Surface Science .575-581. 208-209. (2003)

9. R.J.Nikolic, C.L.Cheung, C.E.Reinhardt, T.F.Wang. Nanotech 2006 Boston , MA, United States, 2006

Chapter 3 Experiment Setup

3.1 Pulsed laser system set up

In our lab, there is a laser source which is used for laser dewetting and pulsed laser deposition. It is 248nm wavelength KrF Eximer laser system with a laser repetition rate of 5 Hz (0.2 sec) and pulse duration of 25 ns.

The main purpose of the system depends on the deposition chamber and connecting pipe with the vacuum system, meters and gas line. For the system involved in this thesis, there is a rough pump, turbo pump, energy meter, high pressure meter and low pressure meter, cubic chamber, target holder and substrate holder, optical elements(lens, mirror), laser system and gas bottles.

3.1.1 Laser system

The laser system is an Excimer Laser LPX 300cc of Lambda Physik Company, and it contains laser head with power supply, vacuum pump, gas filter and control unit. The beam profile is shown in Fig 3.1.

3.1.2 Target

The boron target we selected was purchased from Feldco International Company which is 1 inch in diameter and 1/8 inch in thickness. The target is 99.5% in purity.

3.1.3 Deposition chamber

The vacuum system is part of the core to the whole system. Its edge length is about 6 inches and has six faces which are able to connect with different parts. With careful consideration, the target surface and substrate surface needed to be paralleled since the deposition requires the parallelization of target and substrate due to the character of laser induced plume. Also one face will be connecting to the gas and one will be put on a quartz window with transmission of laser. It is not as convenient as a spherical chamber which is able to connect with outer parts without the limitation of only six faces. The basic chamber design is shown in Figure 3.2(a) (b).

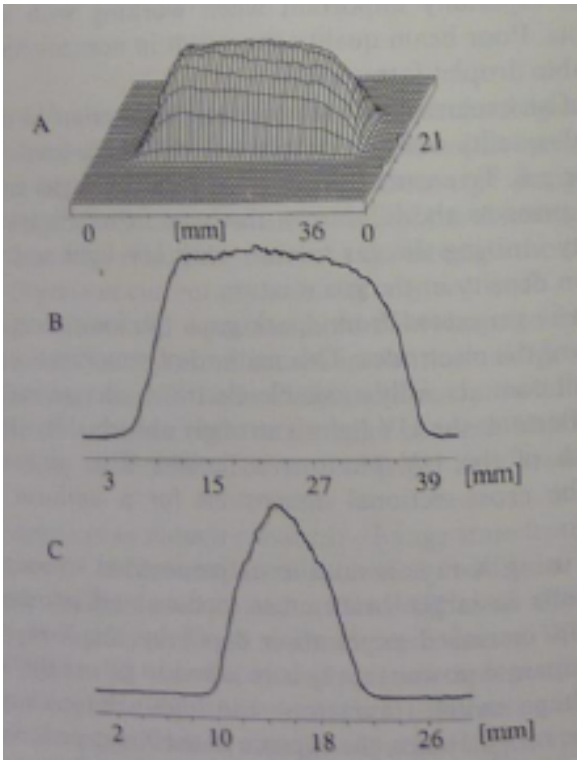


Figure 3.1 Beam Profile obtained from Lambda Physik LPX 300 Laser (A) 3-Dimensional profile, (B) horizontal cross section, (C) vertical cross section

Source: 1.Robert Eason, Pulsed Laser Deposition of Thin Films, Wiley, New York, 2007

In the beginning, we connect the substrate holder to the top face of the chamber and tilt it at 45° parallel to the substrate holder which is also tilted at 45°as shown in Figure 3.2(c).

For easy control of energy density and adding a rotating target holder, the faces of target and substrate loading will be both parallel and horizontal. The center of the face will be aligned with the laser spot. So there are two faces left in horizontal direction. One is for laser window and another is for pumping. The up top side connects to gas or for venting the system. The bottom side is not used at the present progress of the experiment.

3.1.4 Optical parts

The optical parts we use are a reflective mirror and two focus lenses: one is 2 inch in diameter and another is 1 inch in diameter. Both of their focal lengths are 25 cm.

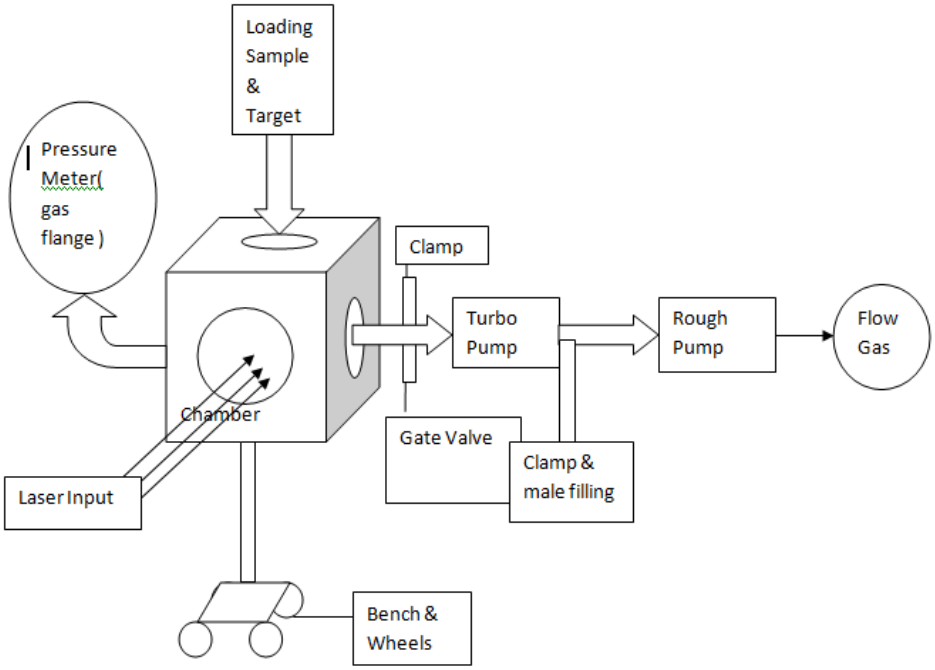
3.1.5 Substrate holder and target holder

It is also important to explore the influence of distance of target and substrate on the growth of a thin film. The substrate holder and target holder are made manually with drilling tools from the MDC substrate holder. In order to adjust the length of holders to change the distance between target and substrate, several holes are drilled onto the holder and a connecting bar, thus it is easy to use the screws to control the distance. See Fig 3.4.

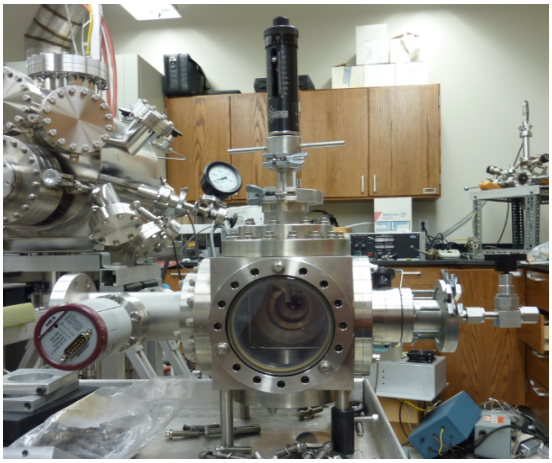
3.1.6 Plasma generation part

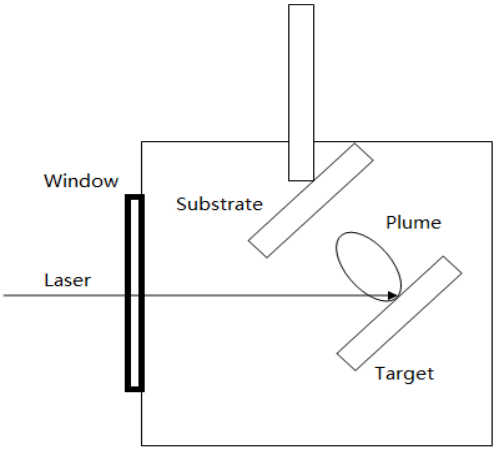
In order to generate plasma, several parts were purchased and assembled, including: electrical feed-through, high voltage generator (Neon transformer), connecting tubes. Also it is

required to drill holes on the electrical feed-through so that the Nitrogen can flow through into the chamber and be ionized by the high voltage. The plasma is generated by high voltage (several hundreds to thousands of volts) ionization of the input gas. It is shown in Fig 3.3.



(a)



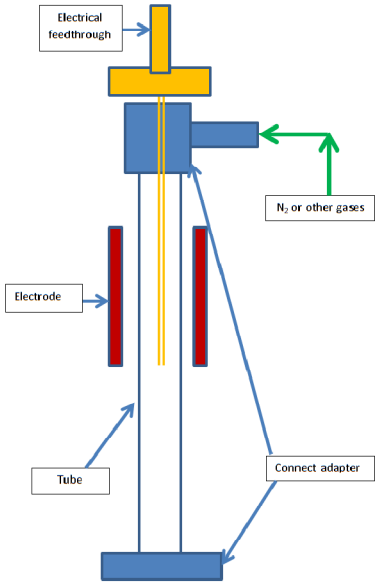


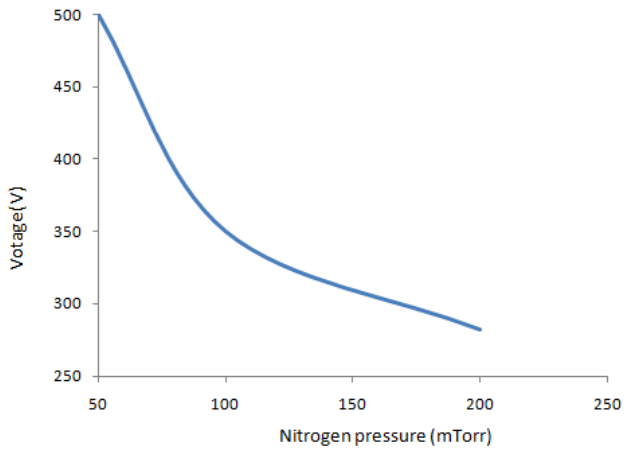
(b) (c)

Figure 3.2 Basic design of the pulsed laser deposition system (a) and system construction (b) target and substrate-target relative positions (c)



(a)





(b) (c)

Figure 3.3. (a) The plasma-generated part (b) Principle for plasma generating (c) Voltage of plasma generation vs. nitrogen pressure

3.2 Experimental processing

3.2.1 Working pressure

The pulsed laser deposition is operating under the pressure around 10^{-6} -10^{-7} Torr. Since the chamber is small it is possible to use rough pump for ~5 minutes to get the working pressure of 10^{-3} Torr for Turbo pump that takes about half an hour obtain to lower the pressure of 10^{-6} Torr. It will take several hours for the pressure to drop to 10^{-7} Torr.

3.2.2 Energy density measurement vs. focus length

When the laser crosses of the aperture, the spot size has a rectangular shape of around 300mm^2. After passing the aperture, it is only 100mm^2. Then beam reflects from the mirror, and there are focus lens on its way to the chamber to decrease its spot size. The energy density increases by decreasing the spot size of laser beam. The spot size is measured from the (dark region) spot hitting on the thermal paper; spot size and the energy density are calculated in Fig 3.5(a), (b). The highest energy density lies around the focal point (25 cm) and is about 4.5 J/cm^2.

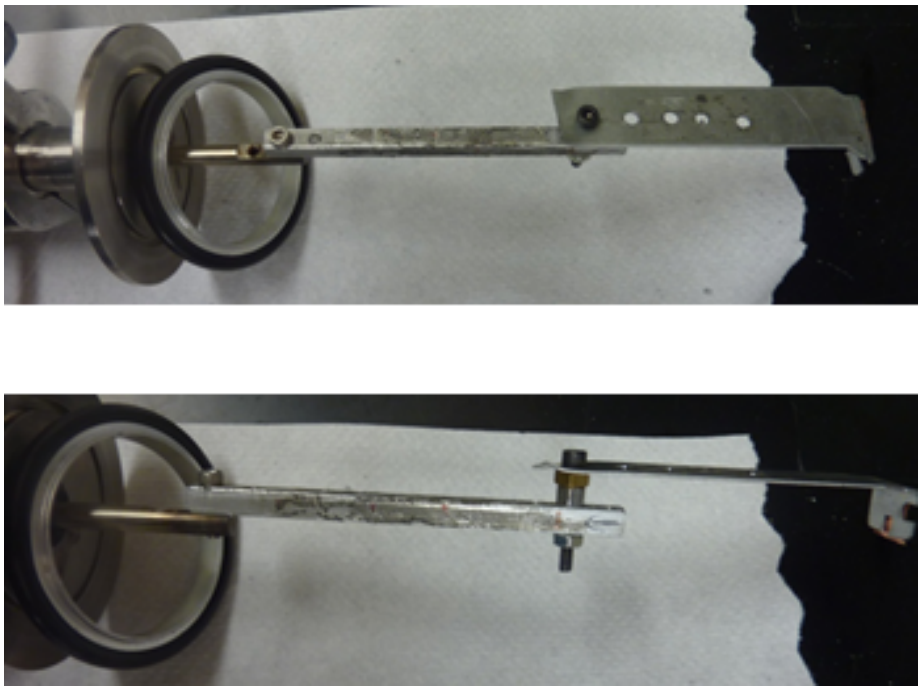
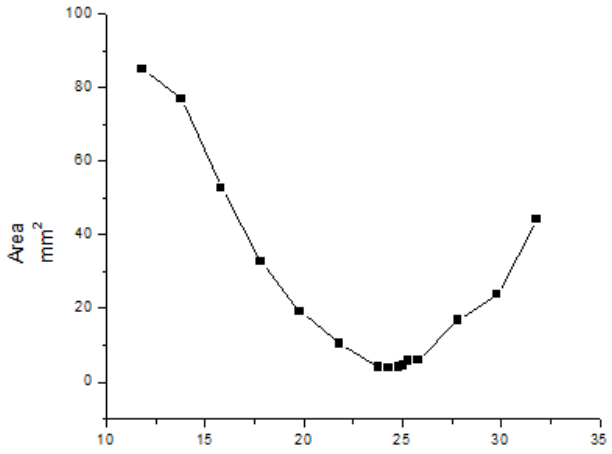
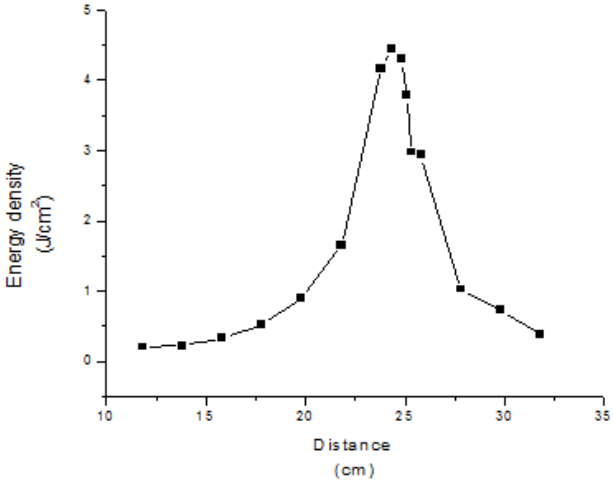


Figure 3.4 The substrate holder with adjustable holes which are 1 cm from each other.



(a)



(b)

Figure 3.5 (a) Spot area vs. distance from target to lens (b) Energy density vs. distance from target to lens

3.2.3 Energy density vs. Plume shape

The plume shape of target material is determined by energy deposited on the surface of material. In the beginning, the energy density is small, resulting in little material evaporation. The absorption of the target material is relatively small, however, when the energy density increases, there is more material ejected resulting in stronger absorption of laser light. When the energy density and absorption reach a threshold point, the plume shape is large and bright. If the energy density continues to increase, the absorption become quite large so that it shielding parts of the laser beam energy, as a result, the shape of plume decreases. As a conclusion, the threshold point is not the point of largest energy density. The plume shape and the energy density are shown in Fig 3.6.

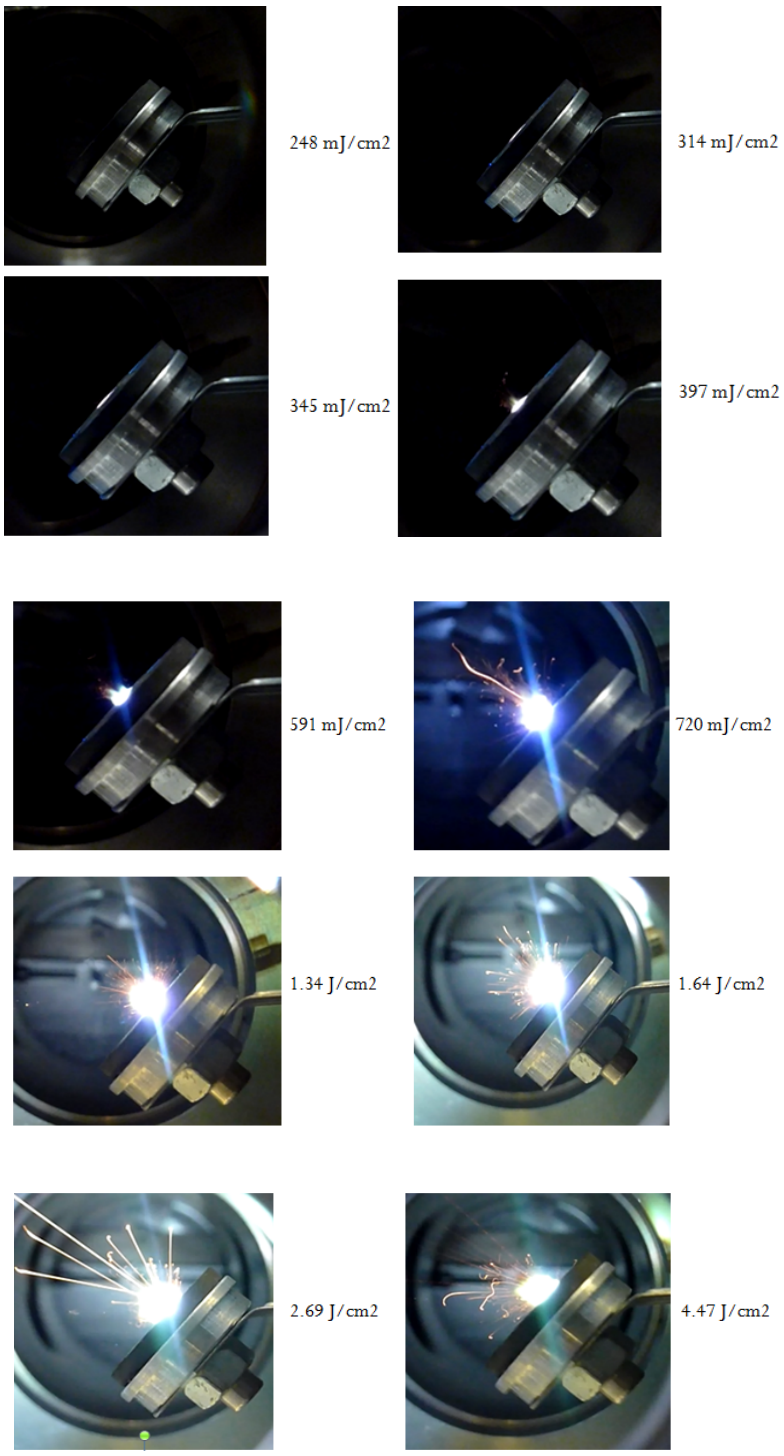


Figure 3.6 Plume shape vs. energy density

3.3 Characterization techniques

3.3.1 Filmetrics Thin Film Analyzer

The F20 thin film reflectometer (Fig 3.7 a) is usually used to measure the thickness and optical constants (n and k) of thin films. Films include oxides, nitrides, resists and polysilicon, optical coatings such as hardness and anti-reflection coatings, flat panel display films such polyimides, resist, and cell gaps, and the various coating used in CD and DVD manufacture. [1]

The F20 uses the transmission and reflection of light by a sample to do the measurement. The light is reanalyzed through a wavelength range. The light reflected by surface of thin film and reflected by interface between thin film and substrate can be strengthened or neutralize partly determined by if these reflected lights are in-phase or out-of-phase. In-phase and out-of-phase interference depends on the light wavelength and thin film material properties like thickness, optical constants. So by inserting the optical properties, the software can fit the thickness precisely.

3.3.2 Grazing angle incident beam X-ray diffraction

The XRD equipment we use is Philips Analytical X'pert XRD system, the purpose of which is to characterize the kind of materials by identifying the characteristic peaks in the x-ray patterns. But the transmittance of X-ray is relatively strong that the data reveal both the peaks of substrate and films if the normal angle is chosen. Therefore, the angle can be adjusted to small enough that the patterns mainly reveal the information of the film. In the grazing angle X-ray diffraction, especially our system, many complicated steps needs to be done including optical

parts set up (mirror and collimator, aperture), 2theta scan (reset the offset of 2theta), z scan (find the distance from X-ray to the surface of sample which will be suitable for X-ray diffraction), Omega scan for the best shape of intensity to determine the z value more exactly. The system is operating in grazing angle mode in Fig 3.6(b).

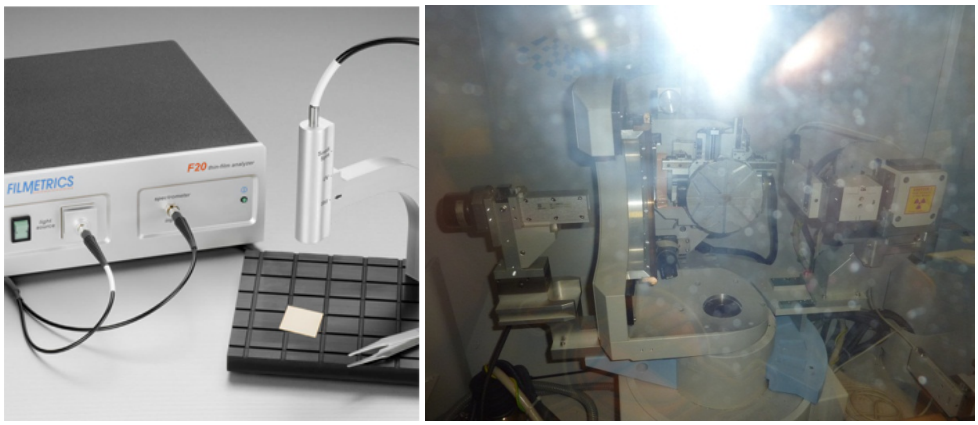
3.3.3 Scanning electron microscopy

When the focused at 0.4 nm-5nm diameter spot, the electron incident beam (typically 0.5keV-40keV) [5]with a specific direction goes into a sample, its direction will change due to the influence of the force with lattice and Coulomb

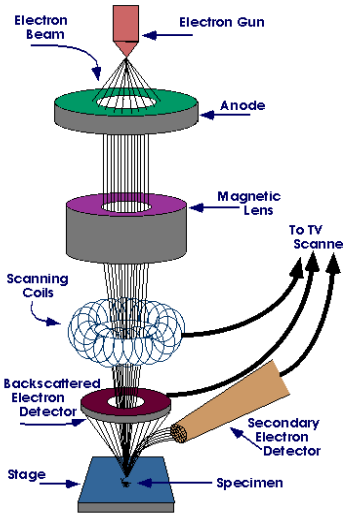
field of atoms. The electron interacts with the sample and generates many signals. The signals, especially secondary electrons and back-scattered electrons are collected by the detectors. See Fig 3.6 (c) The collected signal often reflect the surface and morphology of the sample. The SEM system we use is Hitachi S-4300.

3.3.4 Energy-dispersive X-ray spectroscopy

Energy-dispersive X- ray spectroscopy is mainly designed for the elemental or chemical analysis. It depends on the research of X-rays emitted due to interactions between electromagnetic radiation and material. Because each material has its own specific atomic structure to emits X-rays. As a result, the X-ray can be characterized relative to specific atomic structure.



(a) (b)



(c)

Figure 3.7 (a) Filmetrics thin film analyzer system F20 (b) X-ray diffraction equipment and optical parts set up (c) Principle of SEM

Source: (a) 3.http://www.filmetrics.com/thicknessmeasurement/f20

(c) 4.http://www.purdue.edu/rem/rs/sem.htm

Reference

1.Robert Eason, Pulsed Laser Deposition of Thin Films, Wiley, New York, 2007

2.Fimetrics Thin film analyzer F20 operation manual

3.http://www.filmetrics.com/thicknessmeasurement/f20

4. http://www.purdue.edu/rem/rs/sem.htm

5. http://en.wikipedia.org/wiki/SEM

Chapter 4 Characterization

4.1 Energy density influence

4.1.1 Plume profile and thickness profile

The thickness of a thin film is largely influenced by the energy density of the laser. In this experiment, there is a range of energy density in which the boron thin film is likely to grow on silicon substrate in 3 minutes (900 pulses). In other smaller or even larger energy density, the boron thin film does not deposit on Si, even when is operated for longer time about 30 minutes (9000 pulses).

The film is not uniform due to the property of the plume shape. The plume shape is ellipsoidal and highly directional ($\cos^n\theta$ where $8<n<12$ as θ is between the ejected particle direction and normal direction of the substrate) when its content is propelled to the substrate[1] .The $\cos^n\theta$ function drops nearly one order of magnitude in around 45°-55° and there is almost no material ejected in the 0-30° direction. As shown in Fig 4.1, the center part of plume has much more materials ejected compared to the edge so that there will be much more material deposited on the center of the substrate. It accumulates in the middle point, but little material is found on the edge of the sample.

Therefore in this experiment, the centering point of the sample is measured and compared under different conditions. In the sample in Fig 4.2(a), the thickness distribution is shown in Fig 4.2(b), under a working pressure of $4.3*10^{-6}$ Torr, energy density of about 740 mJ/cm^2 and 900

pulses. The thickness can be fit with an exponential function which will describe the thickness vs. distance from the middle point of the sample under these specific synthesizing conditions.

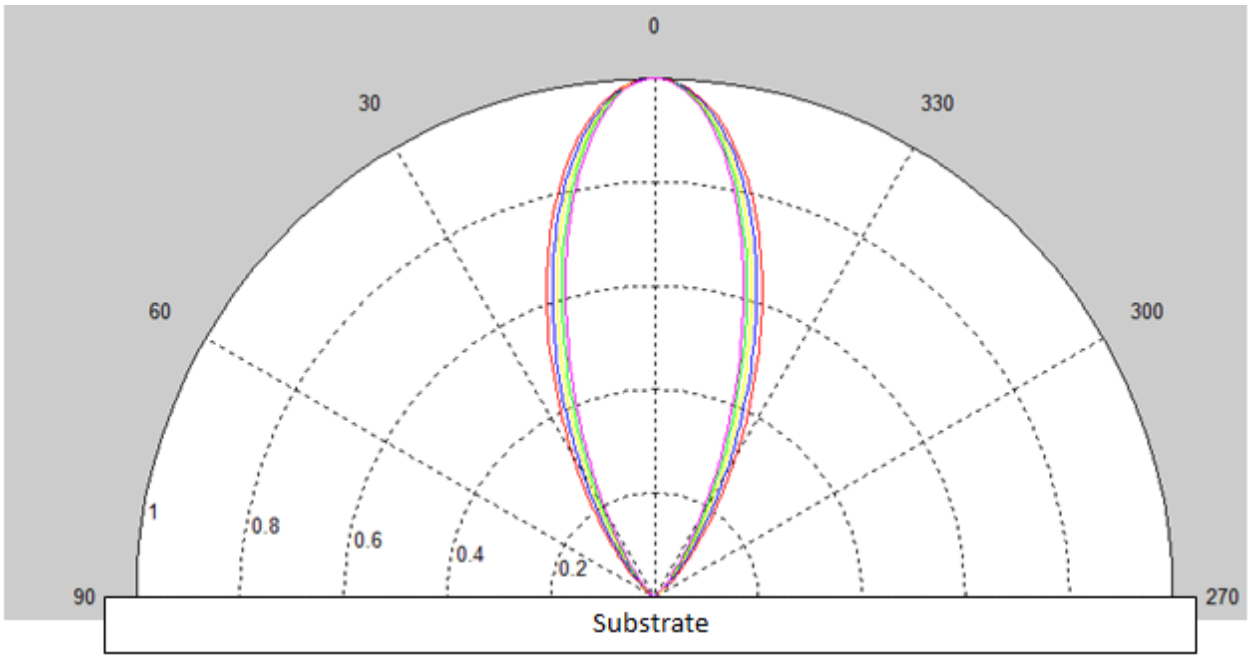
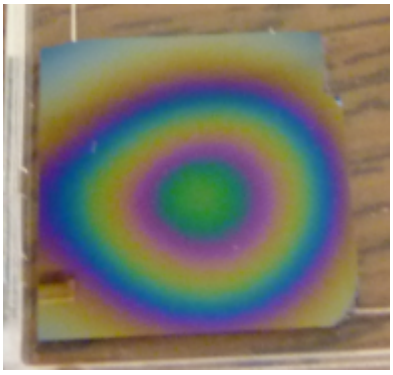
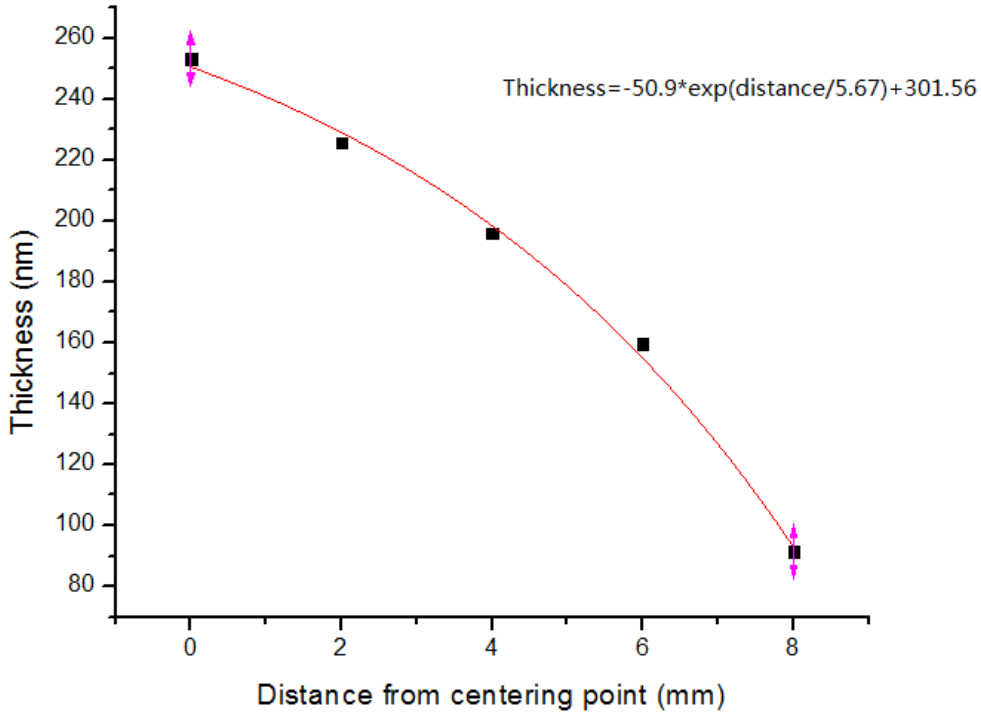


Figure 4.1 $Cos^{n}\theta$ vs. θ and the shape of plume in the polar figure (using Matlab):Red line is $cos^{8}\theta$,Blue line is $cos^{9}\theta$,Yellow line is $cos^{10}\theta$,Green line is $cos^{11}\theta$,Magenta line is $cos^{12}\theta$



(a)



(b)

Figure 4.2 (a) The image of the sample prepared by PLD (b) the thickness distribution on the sample

4.1.2 Samples prepared under different fluence

The series experiment is carried out in two geometrical ways of target-substrate where the target and substrate are in parallel, and the n in the direction normal to target considered as α which is always lies in the plane composing laser beam and substrate holder. The laser beam is always horizontal. So these two sets of geometrical ways of laser deposition are α tilting 45° with the vertical direction and its tilting 45° with the horizontal direction. This is shown in Fig 4.3.

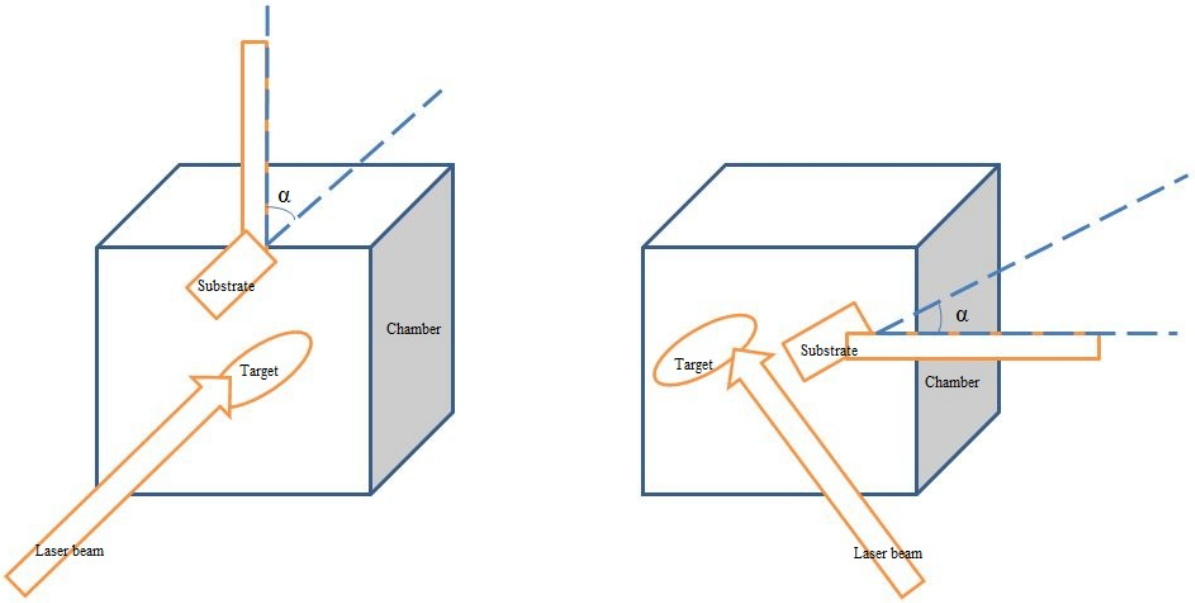


Figure 4.3 Two geometrical ways of target-substrate locations

Various energy densities are tested so as to prepare the boron thin film under threshold energy density point which will enable the laser to evaporate far more material depositing on the substrate. Parameter, such as pressure and middle point thickness are compared in table 4.1 and table 4.2. From the data, we can estimate that the energy density threshold will be around 600

mJ/cm^2 in the vertical direction and around 644 mJ/cm^2 in the horizontal direction. However, from the data in table 4.3, the energy density threshold is shifted due to changing of target and refilling the gas of the laser. Increasing the laser pulse number to 9000 (30 minutes) does not increase the thickness of the boron thin film. This may result from the damage of surface after long pulses, and then the target become resist to be ablated.

Table 4.1 Energy density vs. thickness (tilting with vertical direction)

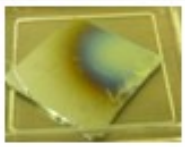
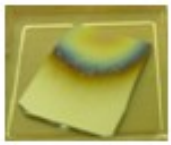
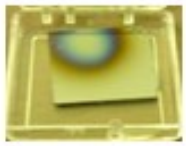
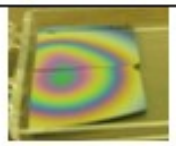
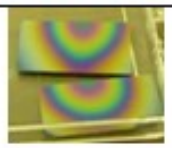
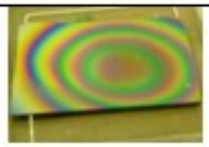
Pressure (Torr)	Energy density (J/cm^2)	Pulses	Thickness at center point (nm)	Photo of samples (silicon substrate)
$3*10^{-6}$	1.52	900	113.64	
$3.8*10^{-6}$	2.88	900	136.05	
$5.5*10^{-6}$	2.88	900	79.61	
$4.3*10^{-6}$	0.74	900	253	
$6.6*10^{-6}$	0.5	900	271.5	
$7.3*10^{-6}$	0.6	900	419.64	

Table 4.1.Continued

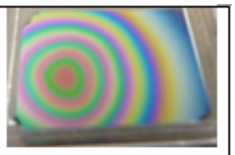
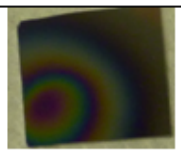
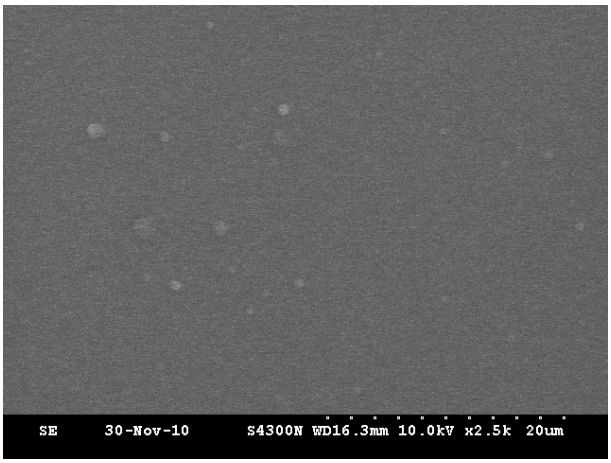
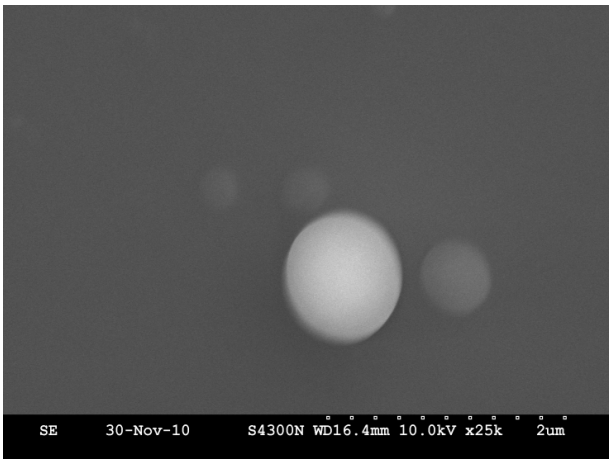
$5.9*10^{-6}$	0.599	900	489.26	
$5.2*10^{-6}$	0.608	900	211.76	

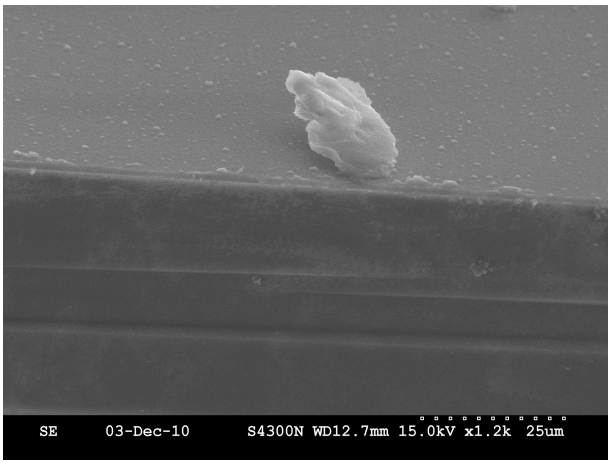
Figure 4.4 SEM images of boron thin film typical morphology prepared with along with the vertical direction



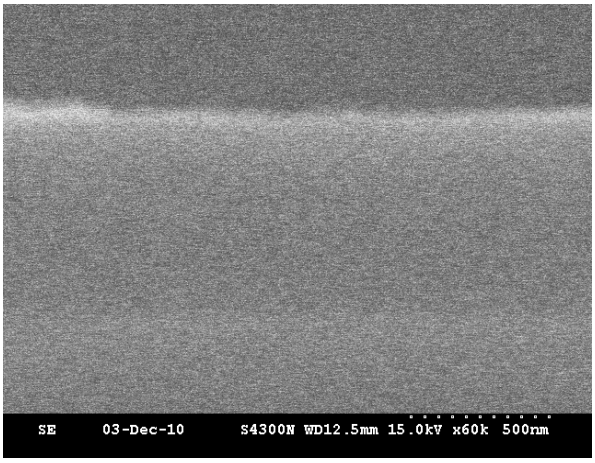
(a)



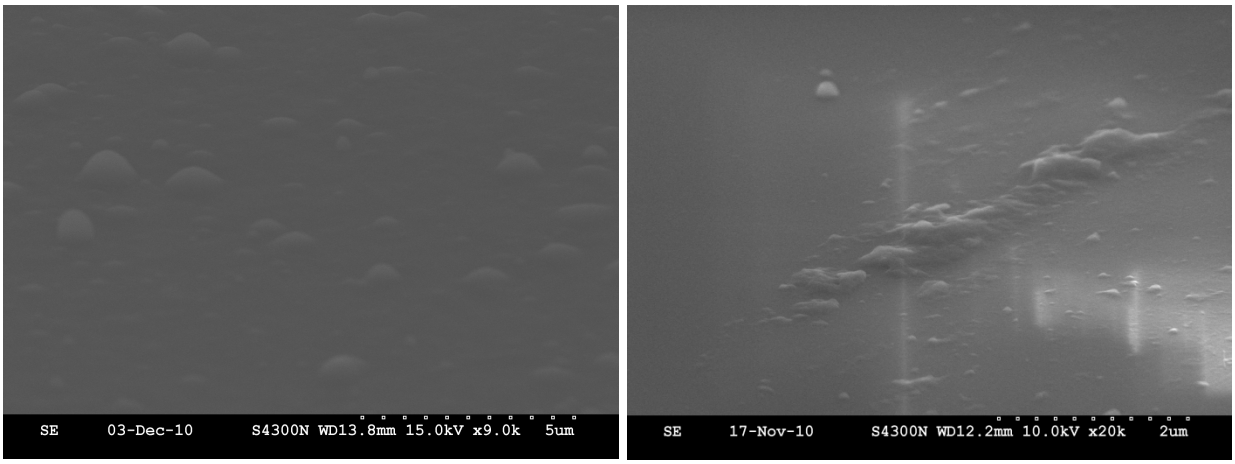
(b)



(c)



(d)



The SEM and cross section SEM images in the Fig 4.4 represent the typical surface morphology of boron thin films prepared by pulsed laser deposition under the condition where the target and substrate are vertical. There existed a lot of droplets as big as 0.1-1 μm in diameter and many islands indicative of the middle process of thin film growth. The thickness of thin film is verified by scanning the cross section of the sample and then comparing the length with standard length.

The thickness in table 4.2 clearly changes with fluence and thickness of the middle point, and can be expressed with an exponential function of fluence in Fig 4.4.

Table 4.2 Energy density vs. thickness (tilting with horizontal direction)

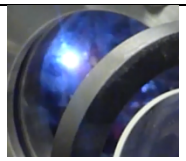
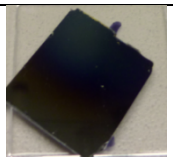
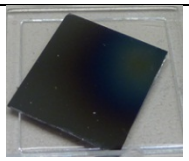
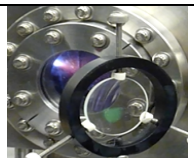
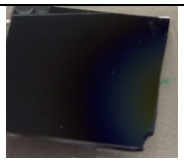
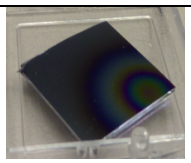
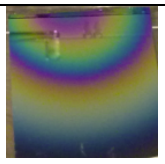
Pressure (Torr)	Energy density (J/cm^2)	Pulse	Center thickness (nm)	Plume shape	Photo of sample (Silicon substrate)
$5.4*10^{-6}$	0.627	900	75.11		
$2.3*10^{-6}$	0.454	900	92.05		
$2.4*10^{-6}$	0.665	900	99.36		
$4.8*10^{-6}$	0.491	900	206.11		
$3.2*10^{-6}$	0.448	900	228.74		

Table 4.3 Energy density vs. thickness (tilting with horizontal direction) after change target and refill the gas

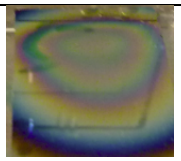
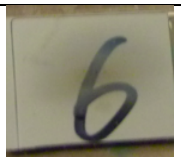
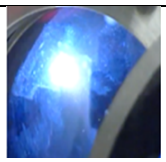
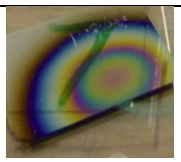
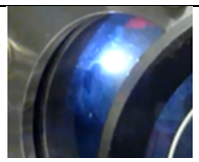
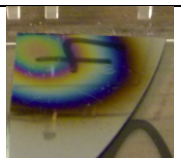
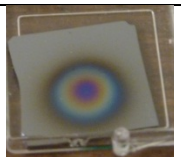
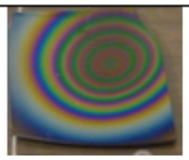
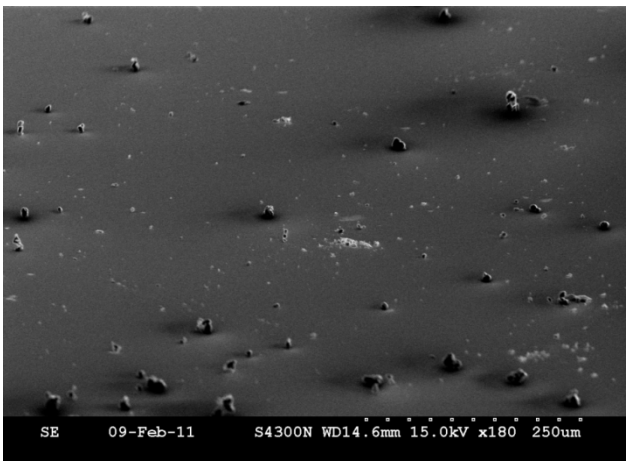
Pressure (Torr)	Energy density (J/cm^2)	Pulses	Center thickness (nm)	Plume shape	Photo of sample (Silicon substrate)
$7.6*10^{-6}$	1.06	900	49.91		
$7.9*10^{-6}$	0.688	900	42.71		
$8.1*10^{-6}$	1.14	900	210.62		
$2.6*10^{-6}$	0.856	900	199.02		
$7.9*10^{-6}$	0.574	9000	130.77		

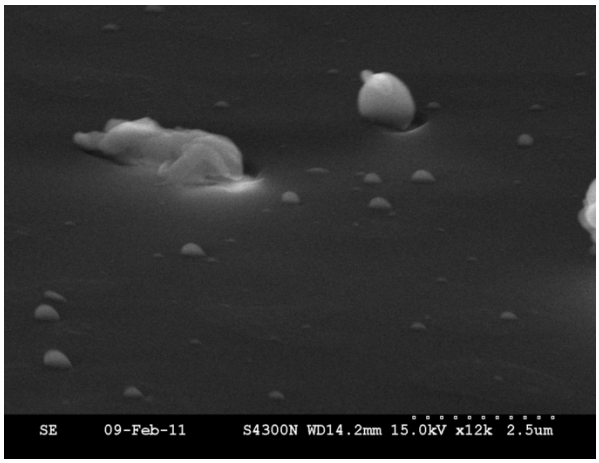
Table 4.3.Continued

$8.7*10^{-6}$	0.644	9000	530.5		

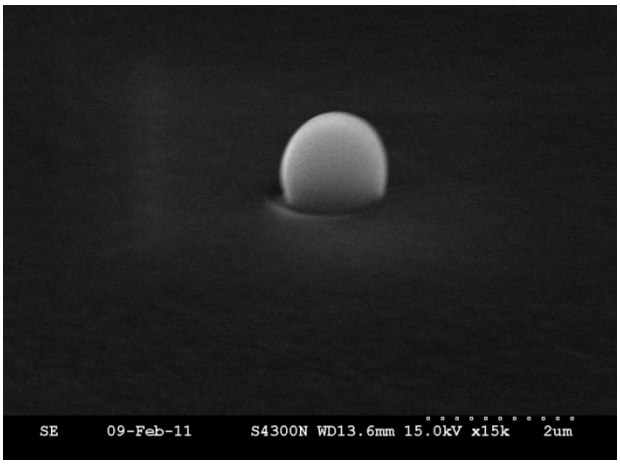
The SEM and cross section SEM images in the Fig 4.5 represent the typical surface morphology of boron thin films prepared by pulsed laser deposition in condition that target and substrate are horizontal. There existed many droplets as large as 0.2-0.5 μm in diameter and many islands as large as 10 μm in diameter for the middle process of thin film growth.



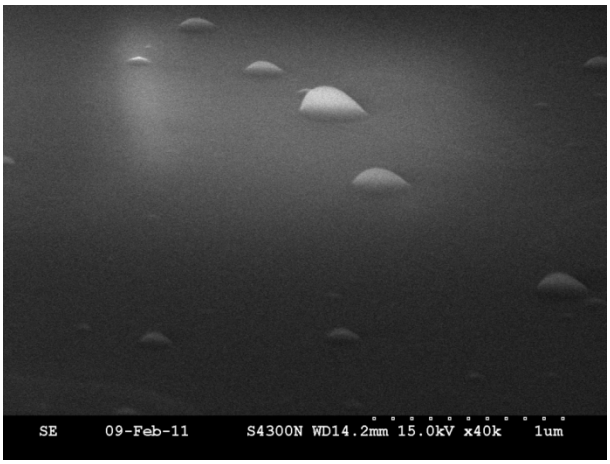
(a)



(b)



(c)



(d)

Fig 4.5 SEM images of boron thin film typical morphology prepared with horizontal direction

4.2 Substrate-target distance influence

In the series experiment of target-substrate distance variation, boron deposits more on the substrate with the closest distance. Then the film appears to decrease both in thickness and width. In order to compare the thickness more conveniently, the same energy density has been chosen to conduct the laser deposition. The results are listed in table 4.3.

The thickness of each sample is plotted with each samples' target-substrate distance. Each sample was measured 5 times at 5 different points beginning with the center point. Each point is 0.5 cm from each other thus a rough thin film surface thickness distribution is graphed in Fig 4.6 to compare the influence of distance on the total thin film thickness.

After getting the data, it is easy to fit the thickness distribution curve with their target-substrate distance with an exponential function:

$$d = \exp\left(3.99 + 2.24 \times l - 0.76 \times l^2\right) \qquad 4.2$$

Which d with unit nm is the thickness at the center point and l in units of cm is the distance between the target and the substrate. The fit curve is presented in Fig 4.7.

Table 4.4 Distance vs thickness

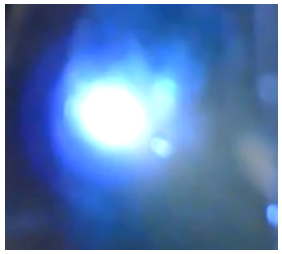
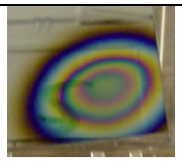
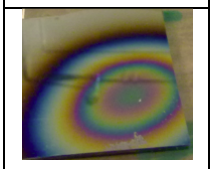
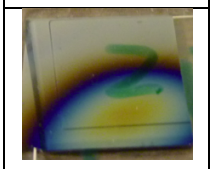
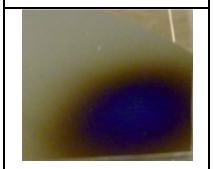
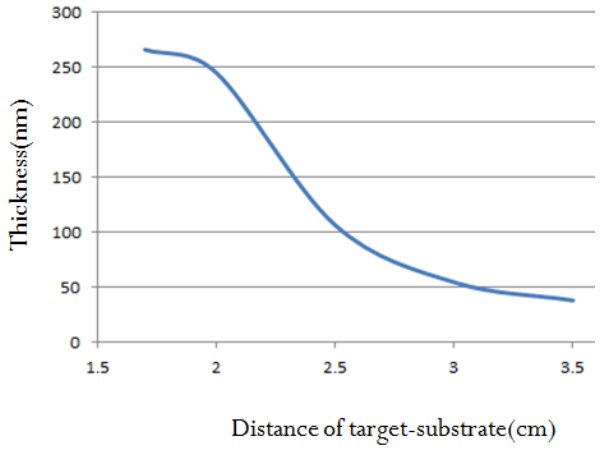
Pressure (Torr)	Energy density (J/cm^2)	Pulse	Distance From target to substrate (cm)	Center thickness (nm)	Plume shape	Photo of sample (Silicon substrate)
$8.3*10^{-6}$	0.594	900	1.7	266.15		
$8.7*10^{-6}$	0.594	900	2	245.12		
$6.3*10^{-6}$	0.594	900	2.5	106.47		
$8.1*10^{-6}$	0.594	900	3	54.59		

Table 4.4.Continued

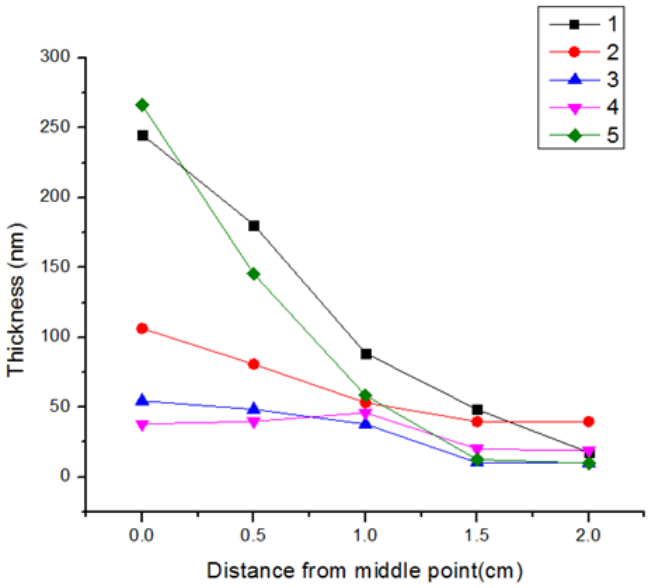
$7.6*10^{-6}$	0.594	900	3.5	38.02		

SEM images are taken for comparing the surface roughness and thin film growth in Fig 4.8.As shown; the one with target-substrate distance of 2 cm appears to have more spherical particles than the next one with greater distance of 2.5 cm. However, the comparison result is not as obvious as the one with distance of 3 cm. It is very clear that in sample 3 there are almost no spherical particles or "droplets" in the sample surface. In sample 4, with distance of 3.5 cm, many small rectangular and triangular particles existed. These might be Si particles mainly resulting from cutting of Silicon wafer. In sample 5 which is the closest distance of 1.7 cm, the material exhibits characteristics that suggest it could be liquid. At the same time, the liquid droplet seems to have very high kinetic energy and travel a short distance on the surface. It becomes stretched that forming a particle shape like "an ellipse ring". These conclusions also can be demonstrated through the cross-section SEM images in Fig 4.9.

The data of experiments are not repeatable sometimes due to many reasons: first, the energy density of laser system is not stable so it is hard to estimate the average value of energy density by eyes. Second, it is hard to estimate the spot size of laser hitting on the thermal paper because some of them do not have a regular shape to calculate the area. Third, the surface of target changes a lot after irradiated of thousands of pulses so that the surface become resisted to ablation.



(a)



(b)

Figure 4.6 (a) thickness of the thin film middle point vs. target- substrate distance (b) the thickness distribution of samples surface vs. distance from middle point of the sample: 1) 2cm, 2) 2.5cm, 3) 3cm, 4) 3.5cm, 5) 1.7cm

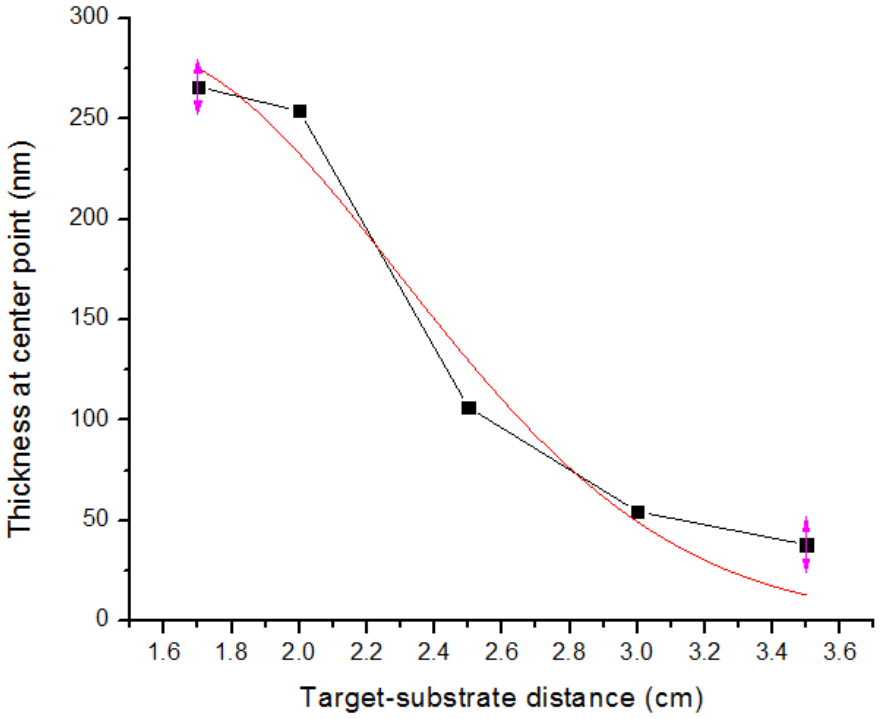
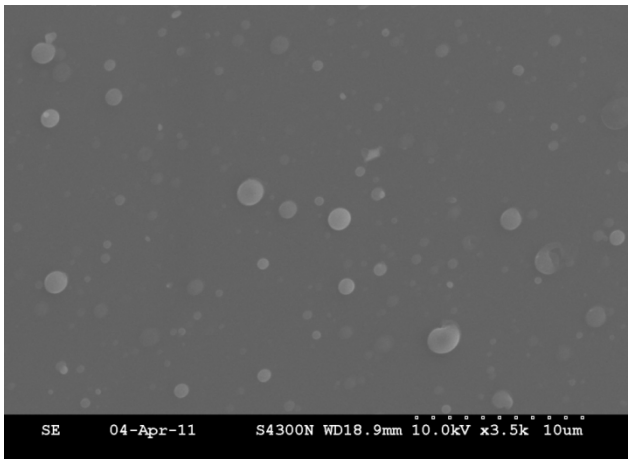
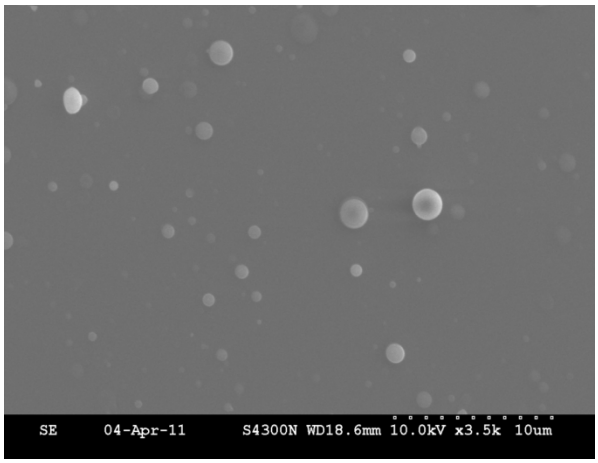


Figure 4.7. Thickness vs. distance curve with exponential function fit

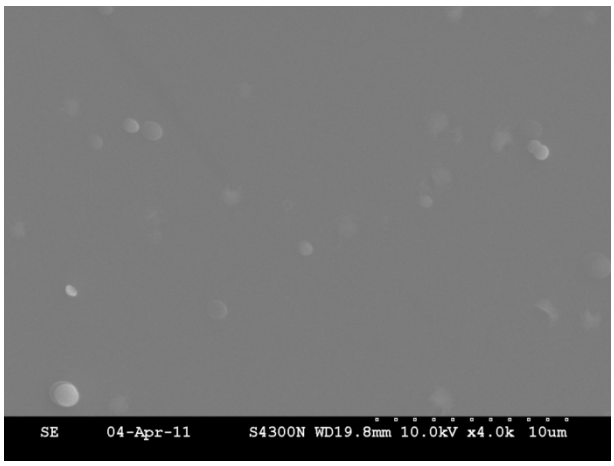
Figure 4.8. SEM images of samples prepared with various target-substrate distances



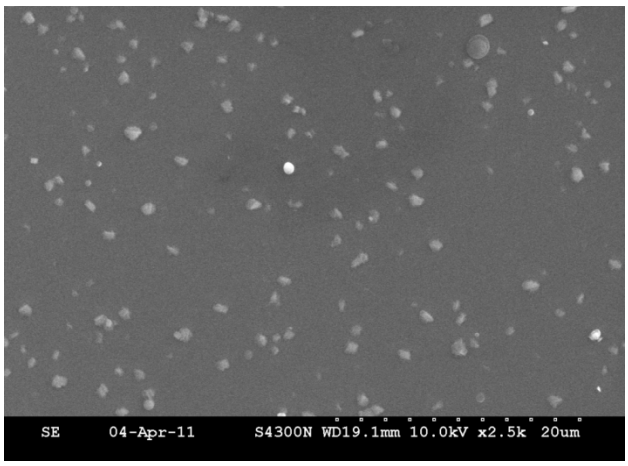
(a) l=2 cm



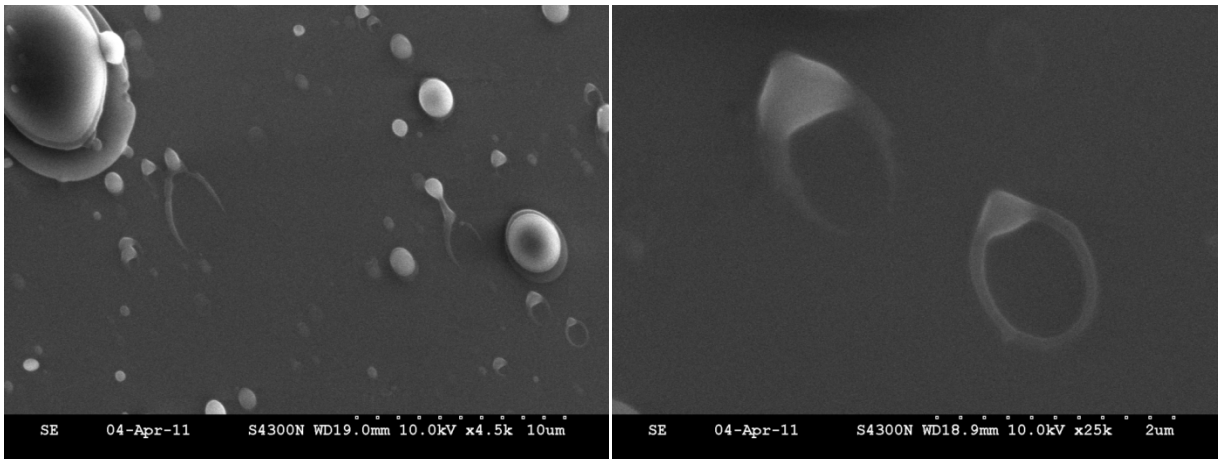
(b) l=2.5cm



(c) l=3 cm

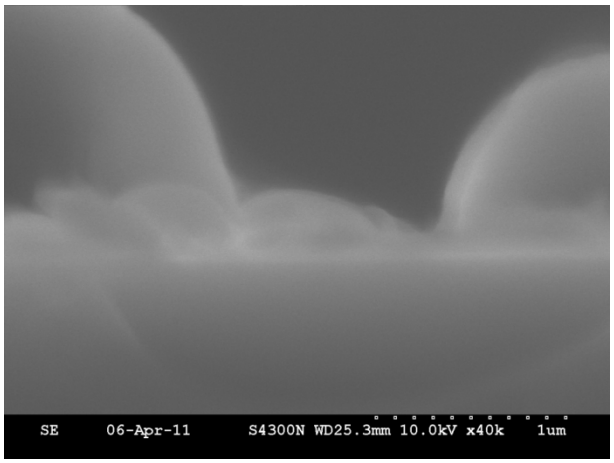


(d) l=3.5cm

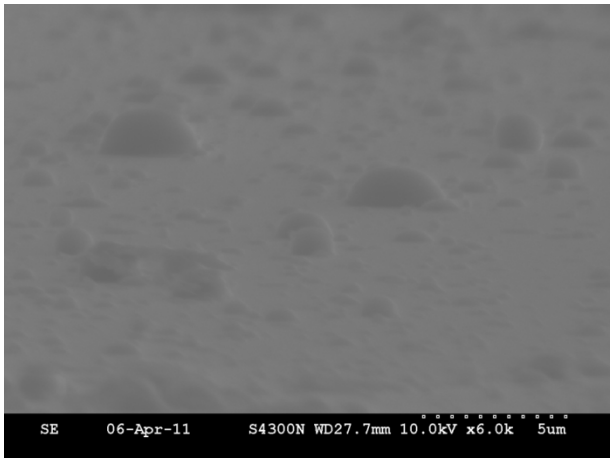

SE 04-Apr-11 S4300N WD19.0mm 10.0kV x4.5k 10um
SE 04-Apr-11 S4300N WD18.9mm 10.0kV x25k 2um

(e) l=1.7 cm

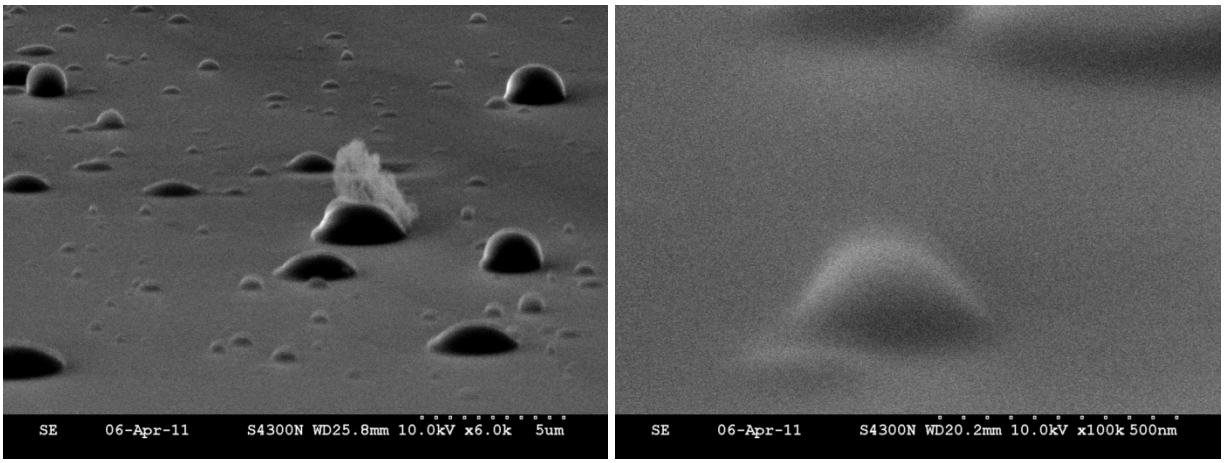
Figure 4.9. Cross-section SEMs comparing with samples prepared under different target-substrate distances



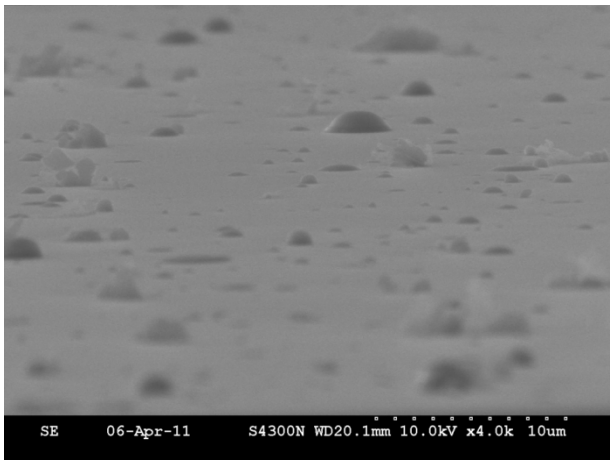
(a)



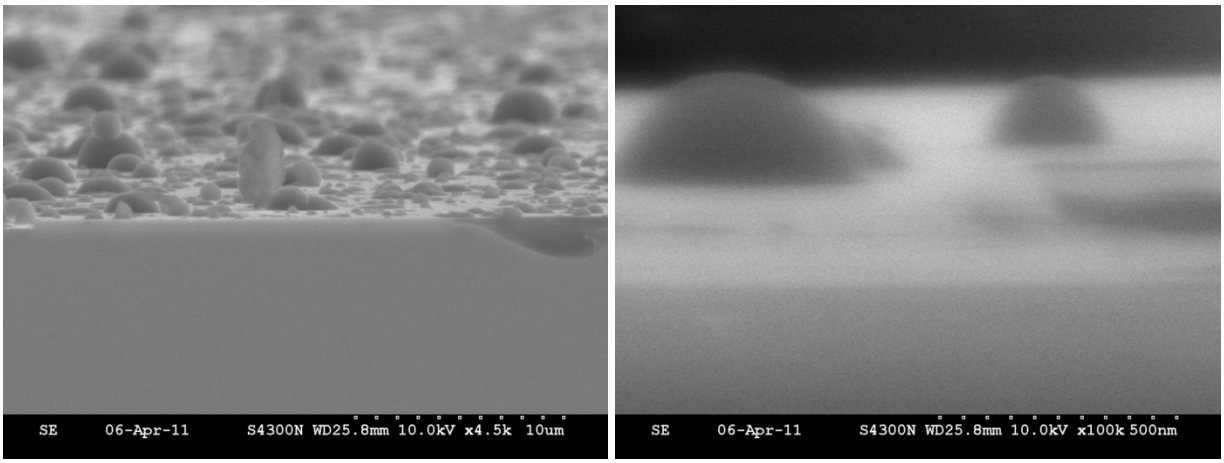
(b)


SE 06-Apr-11 S4300N WD25.8mm 10.0kV x6.0k 5um
SE 06-Apr-11 S4300N WD20.2mm 10.0kV x100k 500nm

(c)


SE 06-Apr-11 S4300N WD20.1mm 10.0kV x4.0k 10um

(d)


SE 06-Apr-11 S4300N WD25.8mm 10.0kV x4.5k 10um
SE 06-Apr-11 S4300N WD25.8mm 10.0kV x100k 500nm

(e)

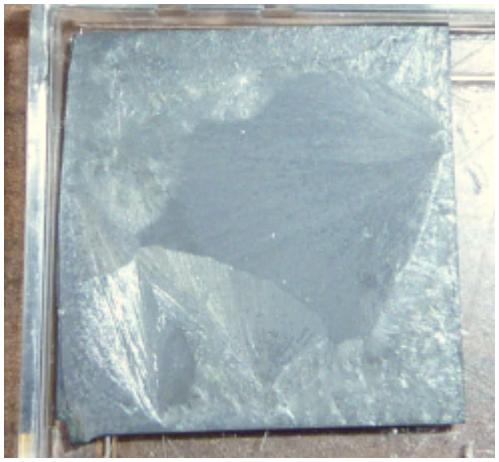
4.3 Annealing study

Since the amorphous boron thin film is obtained via pulsed laser deposition, the annealing process which is conducted in a tube furnace is required to get crystallized boron. Grazing angle X-ray diffraction is used for characterizing and comparing crystallization changes with temperature. After annealing, the color of thin film sample is also changing from colorful circles to gray. The melting point of boron is 2349K, therefore the estimated annealing temperature will be: 50%-70%*$T_{melting\ point}$=0.5-0.7*2076°C=1038-1453°C. At first we anneal the sample for one hour and compare annealing temperatures of 1000°C and 1200°C, and then we anneal another sample for 2 hours and compare annealing temperature at 800°C, 900°C, 1000°C, 1100°C and 1200°C. The data for one- hour anneals is shown in Fig 4.10.

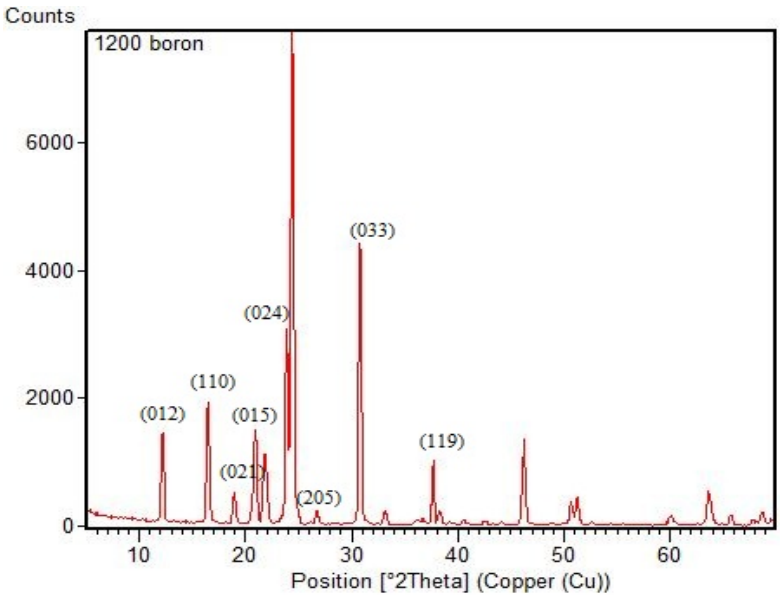
The XRD pattern revealed silicon peaks until the sample is processed under 1200 °C. After fitting the pattern with the boron pattern, the thin film is highly likely to be beta phase of boron with rhombohedral crystal structure.

In Fig 4.11, peak pattern is compared with different annealing temperature, the peaks appears but not obvious even after 1000 °C annealing but are suddenly emerged after 1200°C.

In SEM images in Fig 4.12, apparent crystallization has occurred.

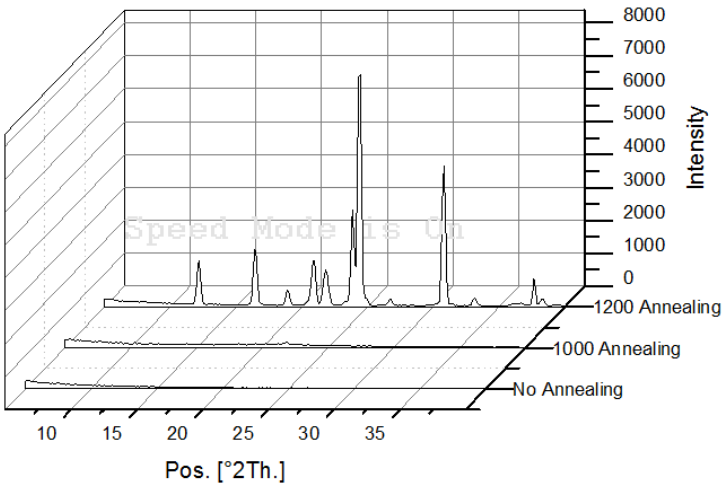


(a)

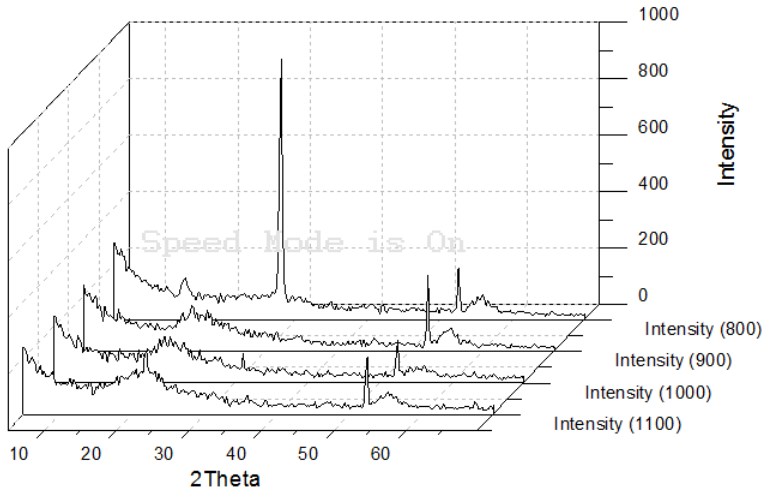


(b)

Figure 4.10. (a)Surface look of the sample annealed after 1200°C (b) The boron peaks existed in the sample annealed after 1200°C



(a)



(b)

Figure 4.11. Comparing of GIXRD pattern of sample (a) annealing at 1200°C, 1000°C and without annealing for one hour (b) annealing at 1100°C, 1000°C, 900°C and 800°C for two hours

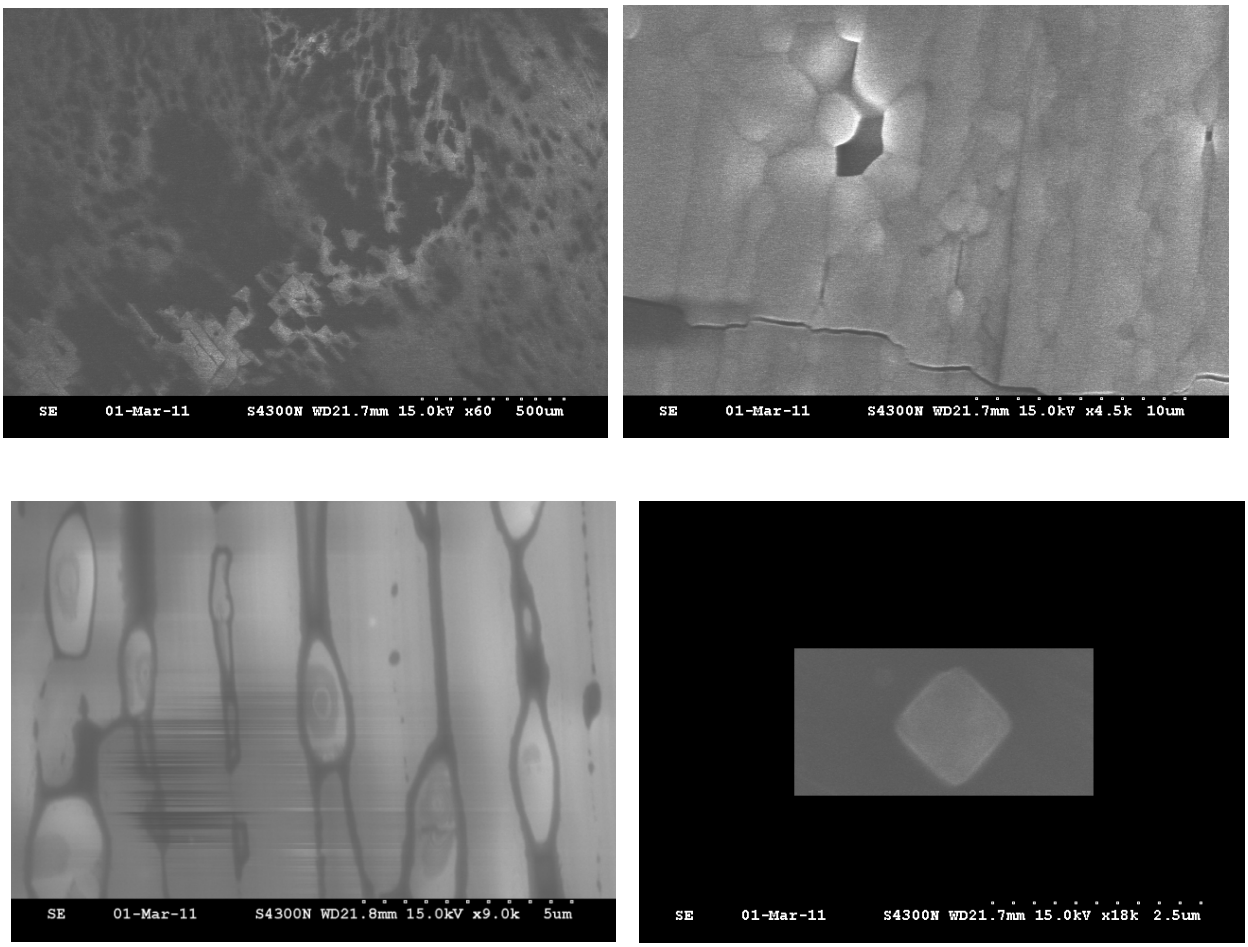


Figure 4.12. SEM images of boron thin film sample after 1200°C annealing for one hour

4.4 Reactive pulsed laser deposition

Boron nitride thin films are prepared by plasma-enhanced pulsed laser deposition. The plasma is generated by a copper tubular electrical feedthrough. The outer part of the tube is connecting to high voltage around 600 V which will ionize the nitrogen between tube and the outside adapter. In the process, the pressure is controlled by manual operation of gate valve. Different pressures of both nitrogen plasma and nitrogen gas are compared as the reactive gas for PLD in Table 4.5 (3mins) at energy density of 666 mJ/cm^2 and Table 4.6 (30mins) at energy density of 582 mJ/cm^2. And the thicknesses are plotted in the Fig 4.13.

Table 4.5 Samples prepared under 3 min (1200 pulses) at 666 mJ/cm^2

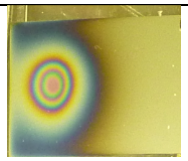
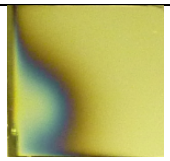
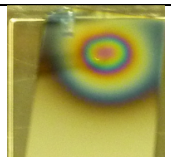
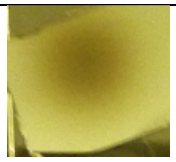
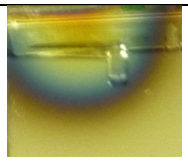
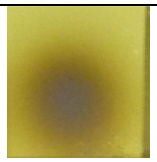
Condition	Thickness (nm)	Photo
60 mTorr Nitrogen plasma	307.6	
60 mTorr Nitrogen gas	77.48	
100 mTorr Nitrogen plasma	198.9	
100 mTorr Nitrogen gas	46.40	
150 mTorr Nitrogen plasma	44.52	
150 mTorr Nitrogen gas	48.07	

Table 4.5.Continued

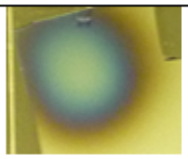
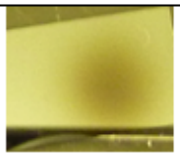
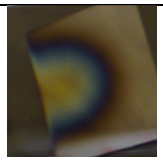
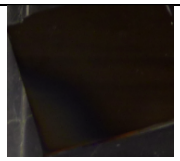
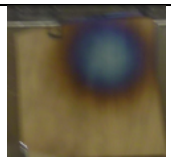
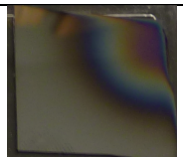
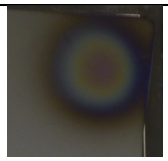
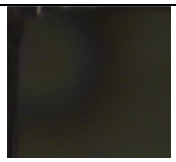
200 mTorr Nitrogen plasma	40.20	
200 mTorr Nitrogen gas	49.11	

Table 4.6 Samples prepared under 30 min (9000 pulses) at 582 mJ/cm^2

Condition	Thickness (nm)	Photo
50 mTorr Nitrogen plasma	75.32	
50 mTorr Nitrogen gas	40.63	
100 mTorr Nitrogen plasma	40.86	
100 mTorr Nitrogen gas	10	
150 mTorr Nitrogen plasma	52.88	
150 mTorr Nitrogen gas	10	

200 mTorr Nitrogen plasma	18.52	

From these data, we could know there is more material deposited on the substrate when plasma is generated by comparing thickness with each other. In nitrogen plasma surrounding, the thickness is 2-4 times larger than in nitrogen gas.

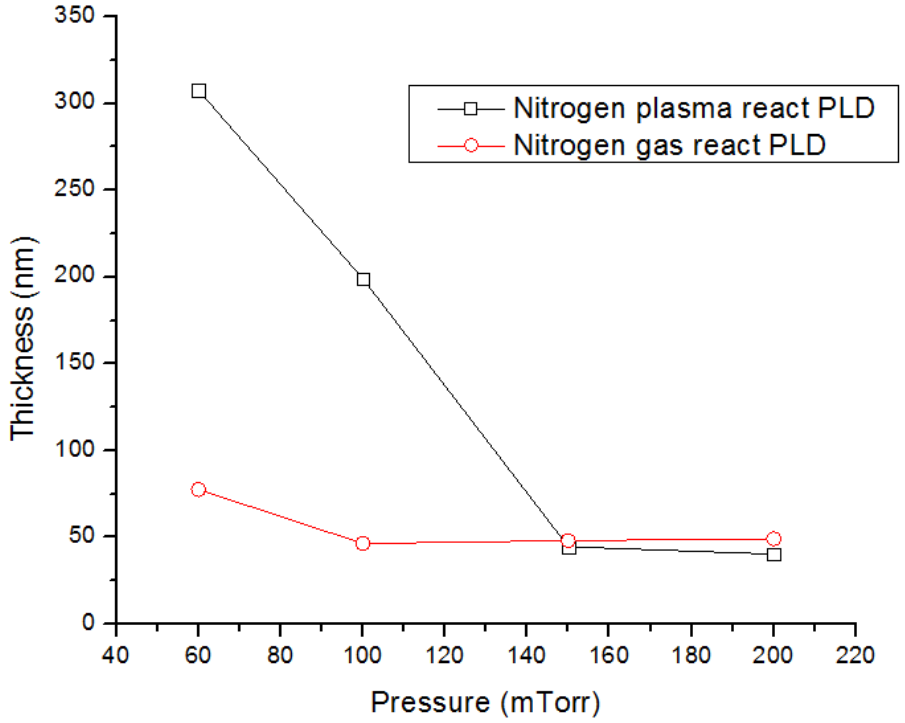


Figure 4.13. Pressure vs. thickness in different conditions

With increasing pressure, the more gas molecular will collide with ablated boron material. Less material will deposit on the substrate. As a result, the thickness of samples prepared under lower pressure is thicker than that prepared under higher pressure. The biggest decrease in thickness happens in 100mTorr-150 mTorr nitrogen plasma part. After that, the thickness keeps constant at about 50 nm. In nitrogen react traditional PLD, the thickness does not change much. It ranges from 70nm-50nm. But after 150 mTorr, it seems neither nitrogen nor nitrogen plasma influence the thickness. As shown in Fig 4.14, the mean free path of 100 mTorr is less than 0.6 cm so that it is smaller comparing to target-substrate distance of 2cm. So the boron molecular cannot reach the substrate to react.

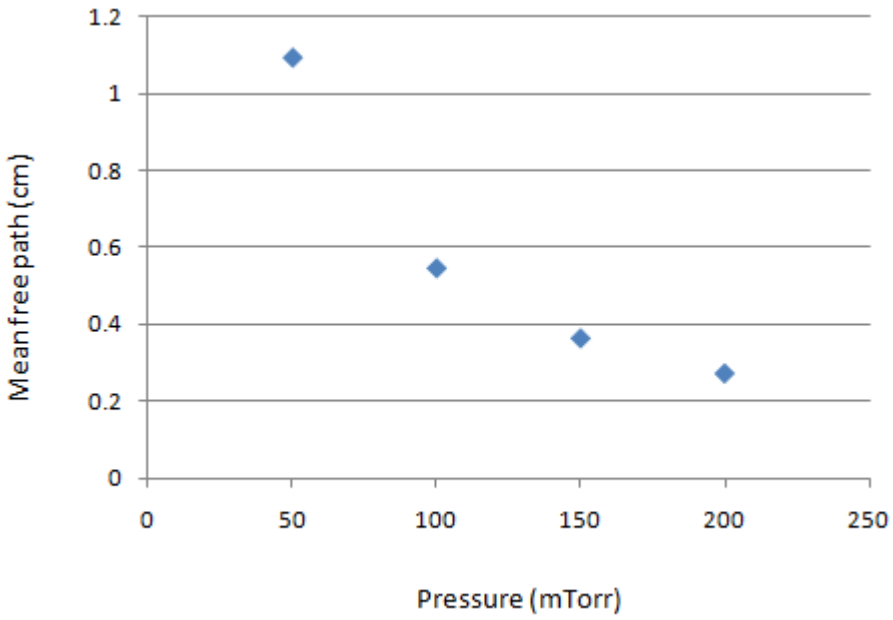


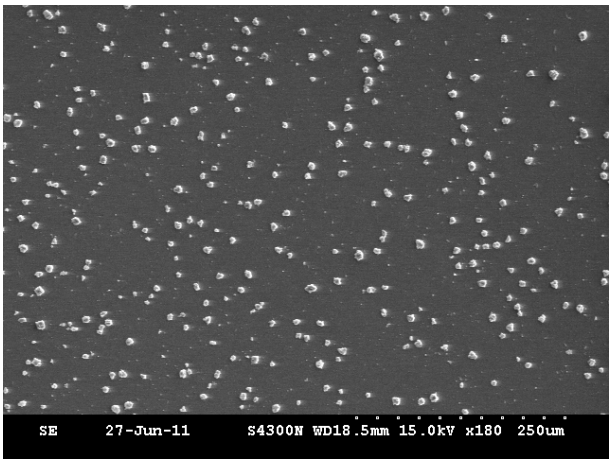
Figure 4.14 Mean free paths vs. pressure

SEM images of samples prepared under different conditions are presented in Fig 4.15(1200 pulses) and Fig 4.16(9000 pulses). In Fig 4.15 (a)-(h), the images shows that with nitrogen

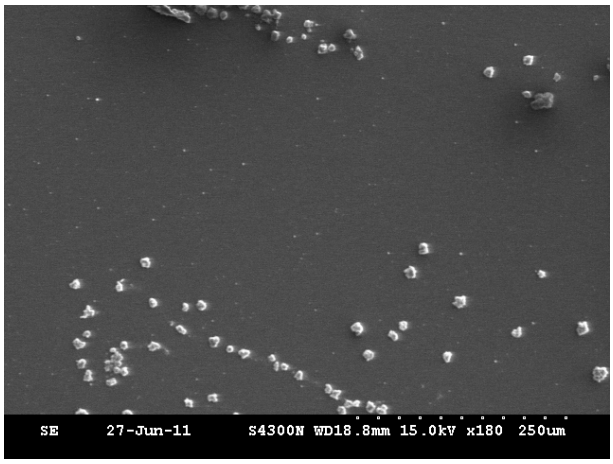
plasma enhanced reactive PLD, samples have decreasing density of larger clusters and sample prepared under 50 mTorr has largest density of clusters with one hundred microns in diameter. The samples prepared in nitrogen gas do not have much different in particle density. In Fig (i)(j), several spherical particles appeared around the clusters around several microns in diameter. In Fig 4.16(9000 pulses)(a)-(g) , clusters in nitrogen reactive PLD is much more than plasma enhanced PLD in pressure from 50 mTorr- 100mTorr. Above 150 mTorr, the clusters density seems the same. In (h)(i), there seems some spider net structure with several microns long deposited on the substrate.

XRD patterns are compared in Fig 4.17 after 1200°C annealing. The peaks are not obvious yet. But patterns of samples prepared in nitrogen plasma have more peaks. At the same location, patterns of samples prepared in nitrogen do not have peaks. It means material did not crystallize in 1200°C annealing. If it is boron, there must be some boron peaks. However, there is not any series of boron peaks that can be identify. So as to explain this, the material deposited is likely to be boron nitride since the annealing temperature of it will be around 1500°C-2100°C which proves no crystallization of boron nitride in relative low temperature. Further proofs need to be found.

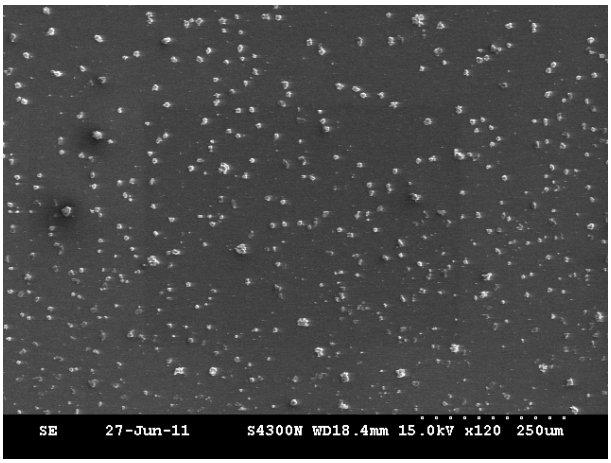
Figure 4.15. SEM images of samples prepare under (a) 60 mTorr plasma (b) 60 mTorr Nitrogen (c) 100 mTorr plasma (d)100 mTorr Nitrogen (e)150 mTorr plasma(f)150 mTorr Nitrogen (g)200 mTorr plasma(h)200 mTorr Nitrogen (i)(j) Typical clusters and spherecial particles of samples



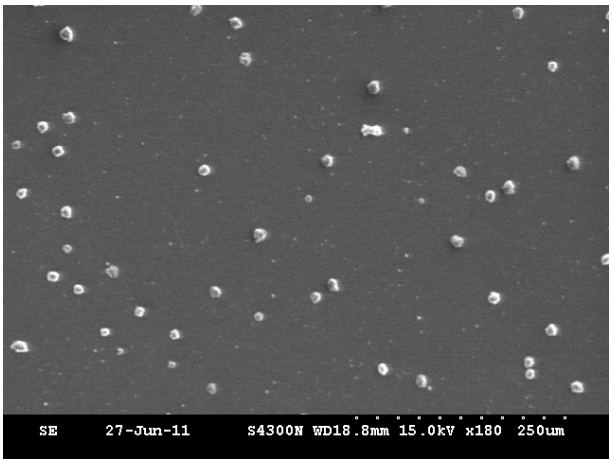
(a)



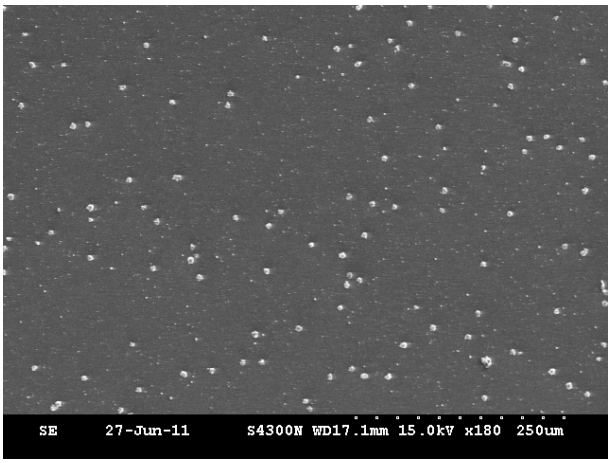
(b)



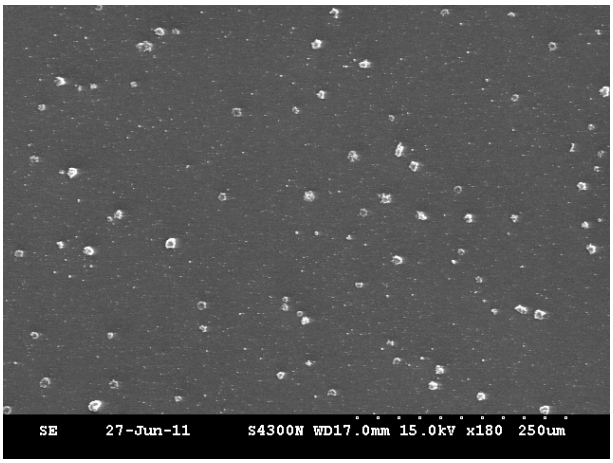
(c)



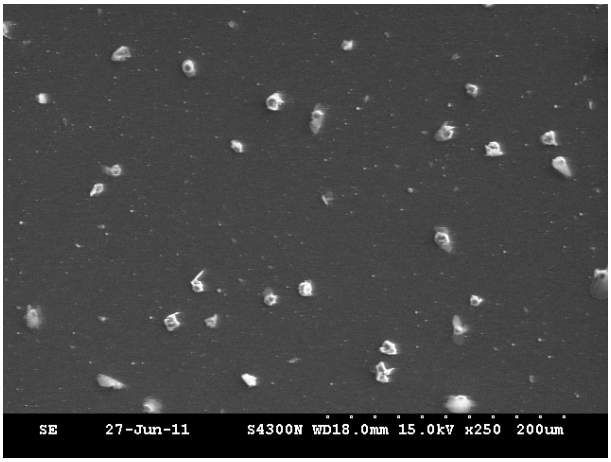
(d)


SE 27-Jun-11 S4300N WD17.1mm 15.0kV x180 250um

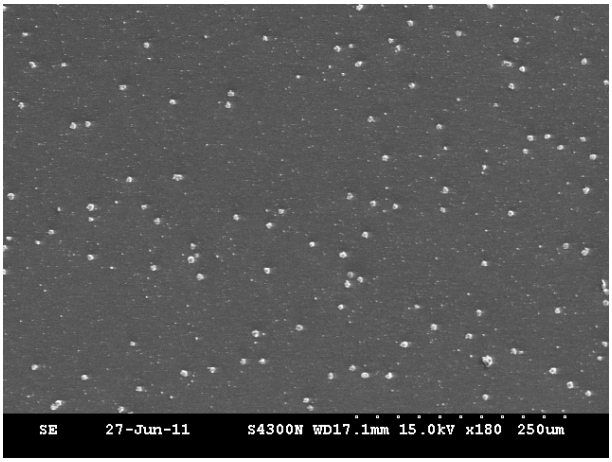
(e)


SE 27-Jun-11 S4300N WD17.0mm 15.0kV x180 250um

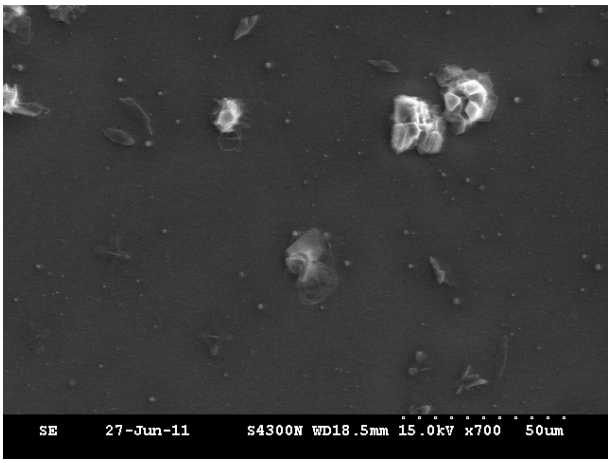
(f)


SE 27-Jun-11 S4300N WD18.0mm 15.0kV x250 200um

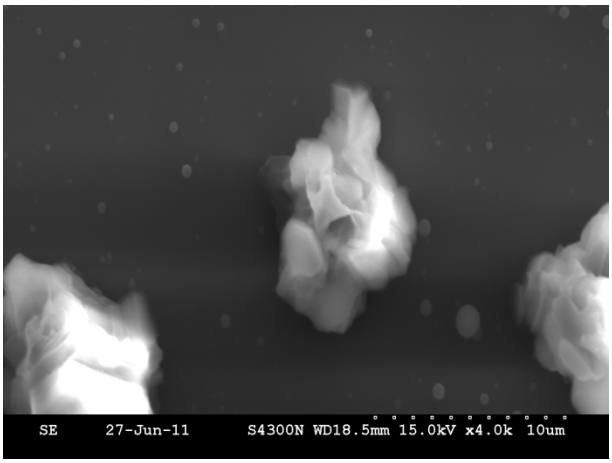
(g)


SE 27-Jun-11 S4300N WD17.1mm 15.0kV x180 250um

(h)

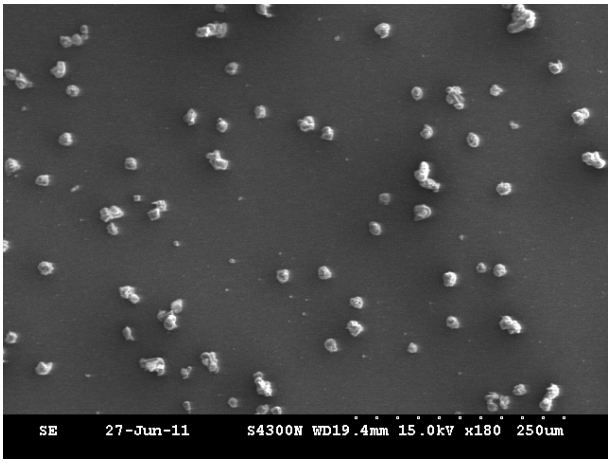

SE 27-Jun-11 S4300N WD18.5mm 15.0kV x700 50um

(i)

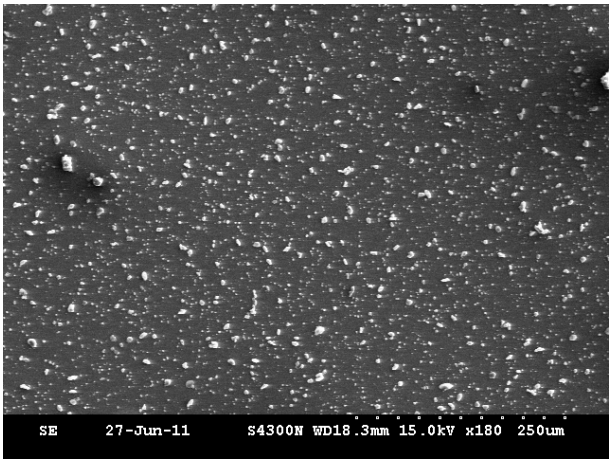

SE 27-Jun-11 S4300N WD18.5mm 15.0kV x4.0k 10um

(j)

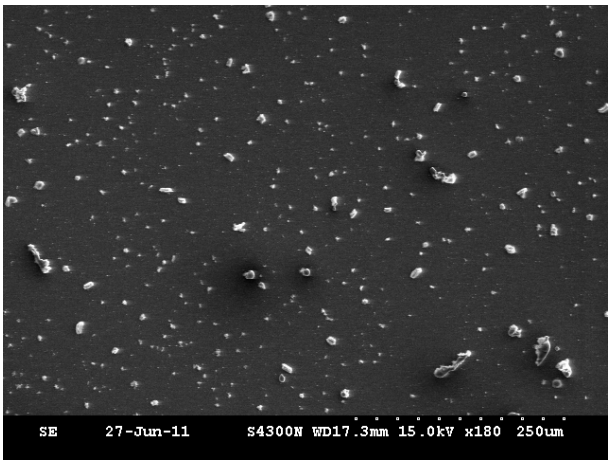
Figure 4.16. SEM images of samples prepare(900 pulses) under (a) 60 mTorr plasma (b) 60 mTorr Nitrogen (c) 100 mTorr plasma (d)100 mTorr Nitrogen (e)150 mTorr plasma(f)150 mTorr Nitrogen (g)200 mTorr plasma (h)(i) Typical clusters and spherecial particles of samples



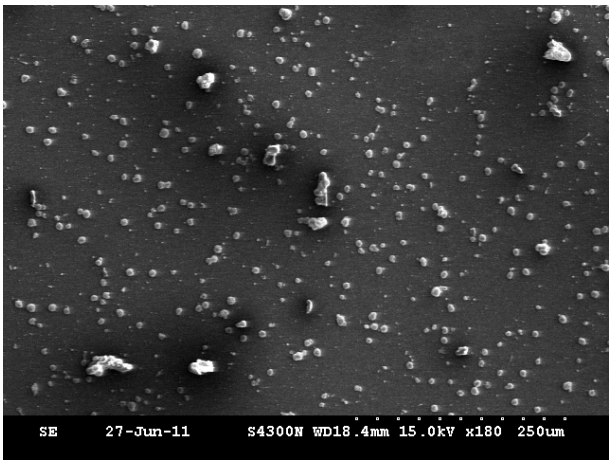
(a)



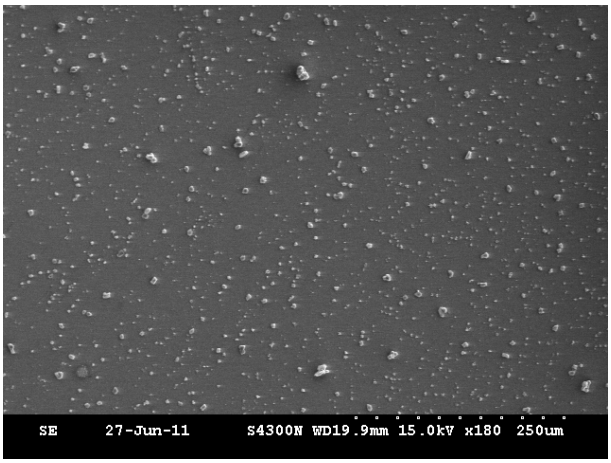
(b)



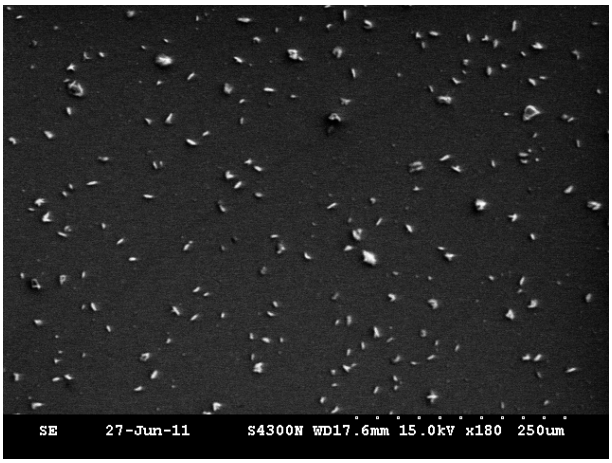
(c)



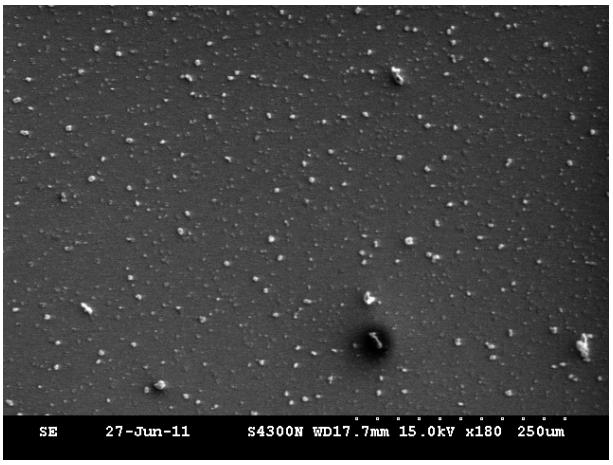
(d)


SE 27-Jun-11 S4300N WD19.9mm 15.0kV x180 250um

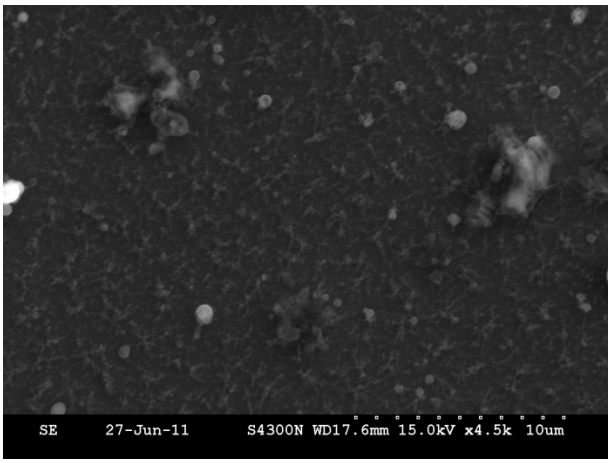
(e)


SE 27-Jun-11 S4300N WD17.6mm 15.0kV x180 250um

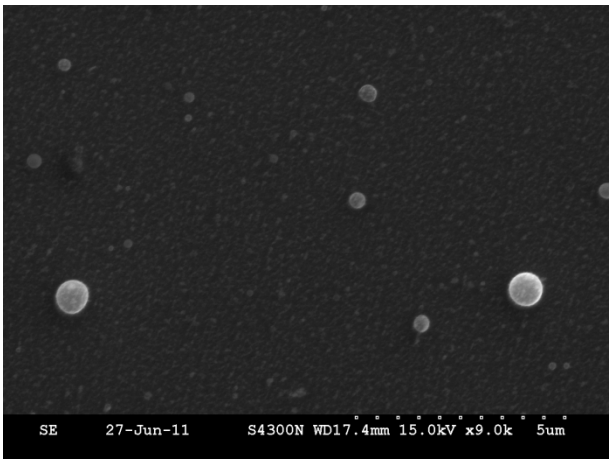
(f)


SE 27-Jun-11 S4300N WD17.7mm 15.0kV x180 250um

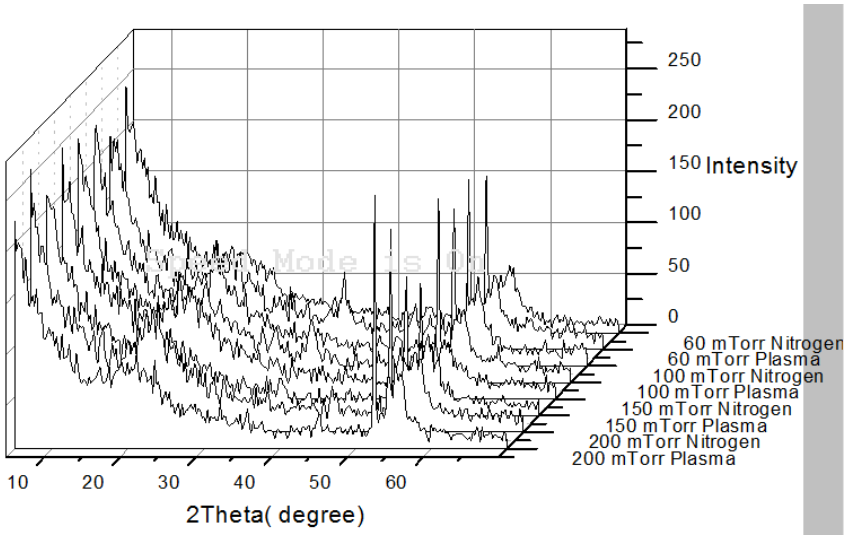
(g)


SE 27-Jun-11 S4300N WD17.6mm 15.0kV x4.5k 10um

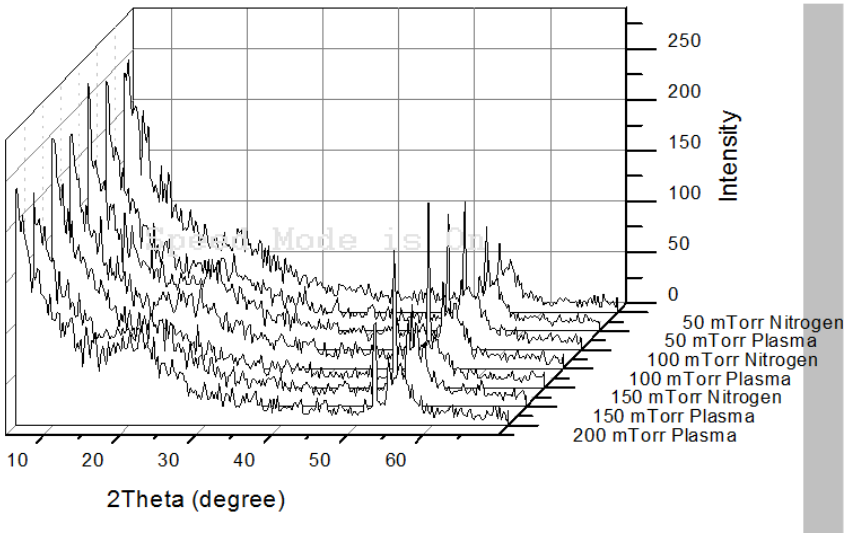
(h)


SE 27-Jun-11 S4300N WD17.4mm 15.0kV x9.0k 5um

(i)

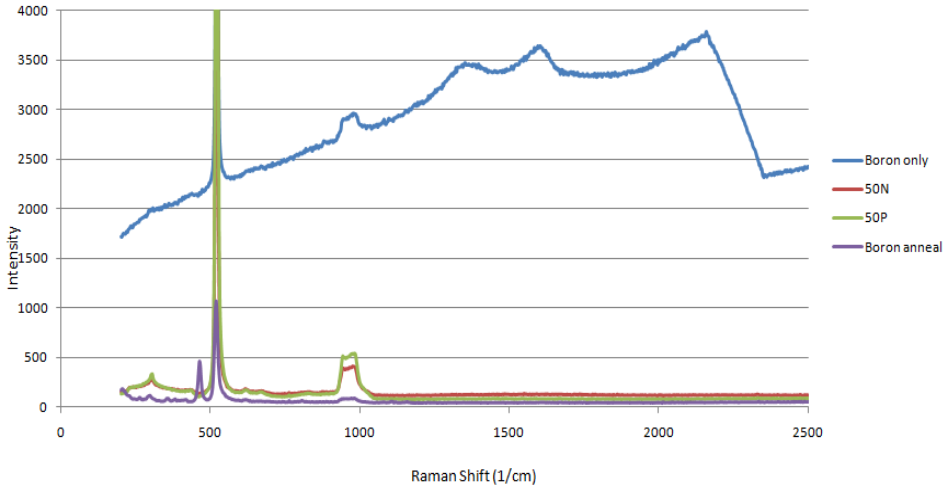


(a)

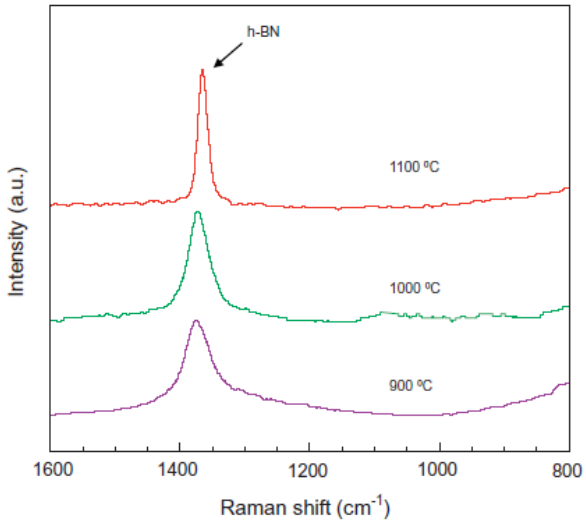


(b)

Figure 4.17 (a) XRD patterns of samples prepared in 1200 pulses (b) XRD patterns of samples prepared in 9000 pulses



(a)



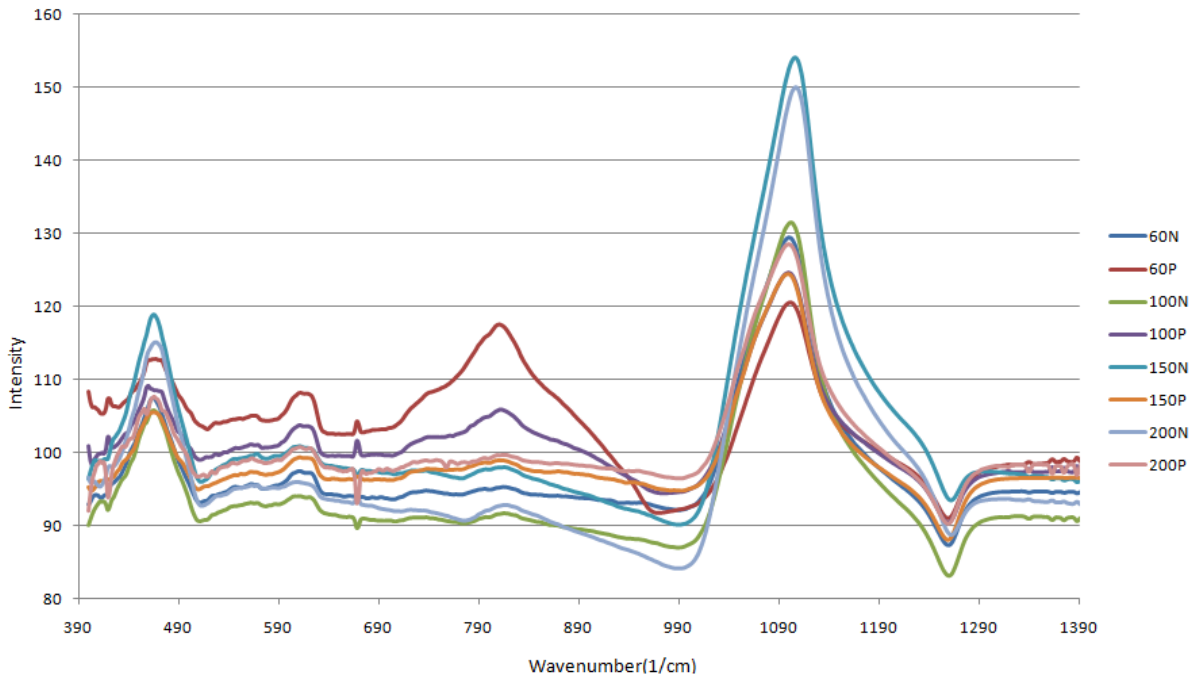
(b)

Figure 4.18 (a) Raman spectra of boron nitride and boron prepared under different conditions (b) Raman spectra of boron nitride prepared under different temperature

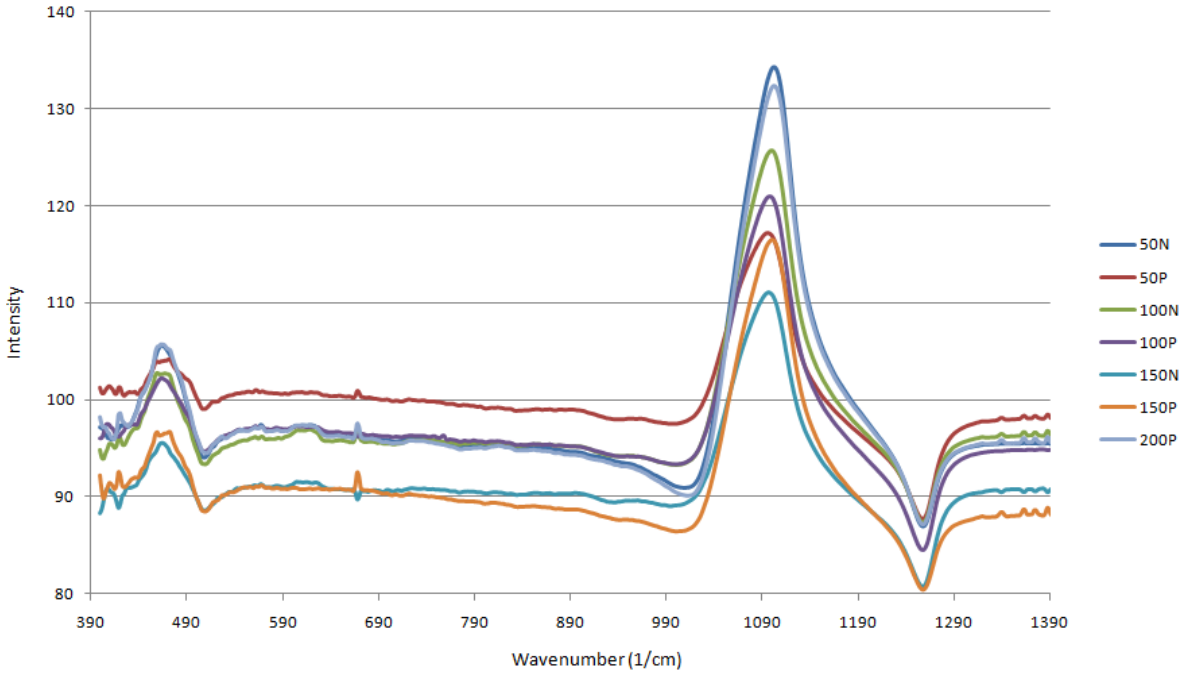
(b)Source : 2. Jun Sheng Li, Chang Rui Zhang, Bin Li. Applied Surface Science.257. 7752–7757.2011

Figure 4.19 FTIR spectra of samples: (a) samples prepared under 1200 pulses (b) samples prepared under 9000 pulses (c) boron sample after annealing (d) FTIR spectra in literature

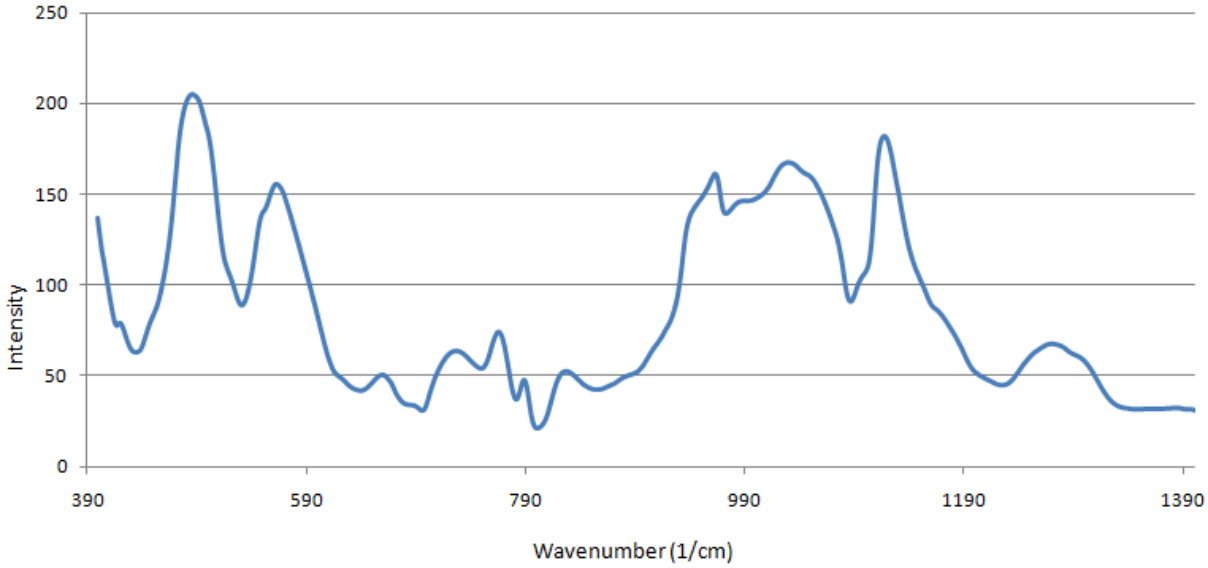
(d)Source : 3.Jos´e E. Nocua, Fabrice Piazza, Brad R.Weiner, and GerardoMorell. Journal of Nanomaterials, 2009, 429360, 1-6, 2009



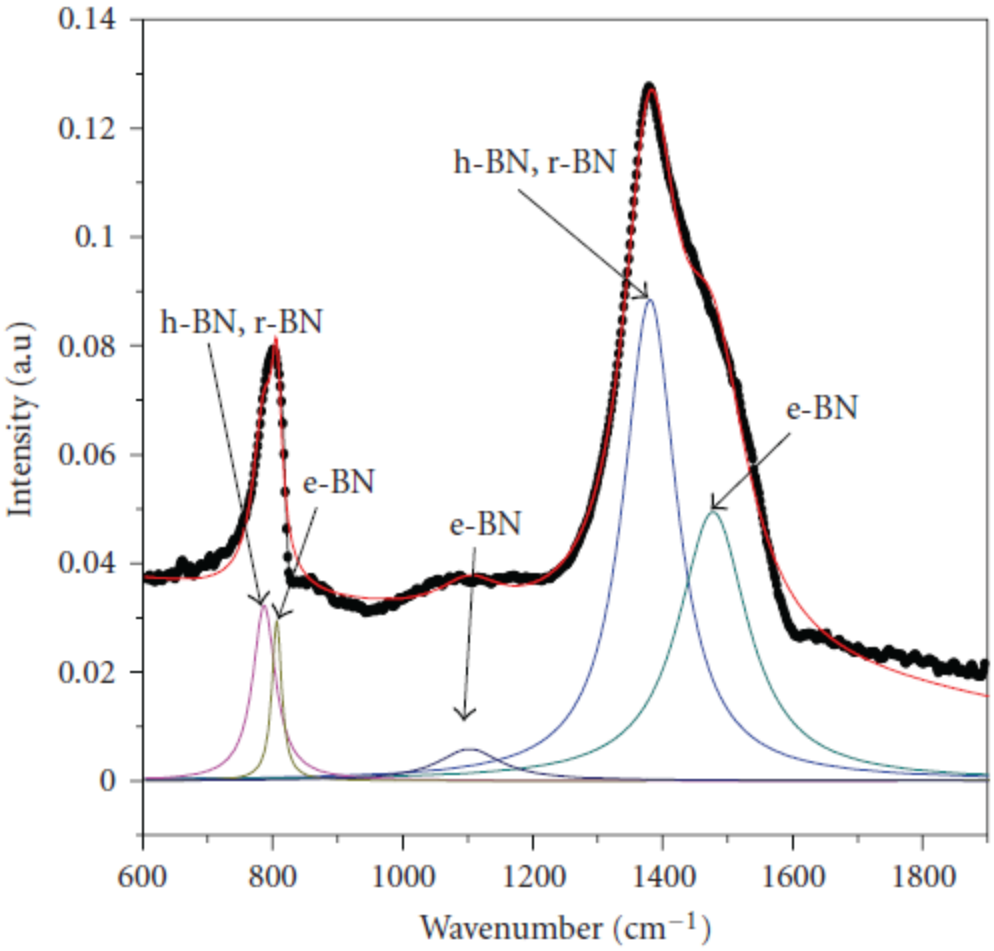
(a)


140
130
120
110
100
90
80
Intensity
390
490
590
690
790
890
990
1090
1190
1290
1390
Wavenumber (1/cm)
50N
50P
100N
100P
150N
150P
200P

(b)


250
200
150
100
50
0
Intensity
390
590
790
990
1190
1390
Wavenumber (1/cm)

(c)


0.14
0.12
0.1
0.08
0.06
0.04
0.02
0
Intensity (a.u)
h-BN, r-BN
h-BN, r-BN
e-BN
e-BN
e-BN
600
800
1000
1200
1400
1600
1800
Wavenumber (cm^{-1})

(d)

Raman spectra data are plotted in Fig 4.18. Boron annealing sample is also scanned for comparing. Peaks in raman shift around 500 and 1000 cm^{-1} is silicon peak. Boron without annealing sample shows a large background. Boron annealing sample shows a peak around 460.944 cm^{-1} besides silicon peaks. While samples prepared under nitrogen gas and plasma both only show a very tiny peak around 457 cm^{-1} besides silicon peaks, it does not fit the data of boron nitride peak around 1400 cm^{-1}. Also if the film is amorphous, it is hard to find peaks in the Raman spectroscopy.

FTIR-(Fourier transform infrared spectroscopy) spectra data are plotted in Fig 4.19(a)-(d). Comparing to other samples, annealing boron sample shows many peaks 480,557,651, 759, 819, 958, 1112 cm^{-1}. And samples prepared under plasma and nitrogen gas did not show much peaks after annealing. Another possible material will be silicon dioxide which has a peak around 1100. But still there are no Raman peak and XRD peak shows there is silicon dioxide. So excluding other candidate material, the thin film prepared is highly likely to be boron nitride thin film with FTIR data.

In Fig 4.19(a), sharp peaks are present in around wave number of 800 and 1100 cm^{-1} in samples prepared under 1200 pulses. In 800 cm^{-1}, the peak seems to be h-BN (hexagonal boron nitride), r-BN (rhombohedral boron nitride) or e-BN (an allotropic phase of boron nitride which is reported to be prepared via shock wave compression through the way of explosion)[4]. And around 1100 cm^{-1}, the peak should be e-BN. The samples prepared under different plasma pressure shows an phenomenon: peak around 1090 cm^{-1} increases and shifts to left sharply but peak around 800 cm^{-1} decreases sharply with increasing the pressure; Samples prepared under

different nitrogen gas pressure shows peak decreasing around 1090 cm^{-1} and decreasing around 800 cm^{-1}. The intensity of sample prepared in plasma is much larger than that prepared in nitrogen around 800 cm^{-1}, but smaller than that prepared in nitrogen around 1090 cm^{-1} overall. Therefore, the r-BN, h-BN and e-BN exhibit a competitive growth with each other and also they do have a favor growth condition. It is easy to conclude that in plasma enhanced PLD, h-BN and r-BN prefer to grow in low pressure and e-BN does not like to grow. It is opposed in high pressure. In nitrogen gas enhanced PLD, h-BN and r-BN are not willing to grow but e-BN is likely to grow in low pressure. It is also opposed in high pressure. In general, h-BN and r-BN are willing to grow in plasma enhanced PLD rather than gas enhanced PLD. And e-BN prefers gas enhanced PLD.

However, in Fig 4.19 (b), under 9000 pulses, the peaks around 800 $^{-1}$ disappeared but peak around 1100 cm^{-1} still exists. It means h-BN and r-BN are transformed into e-BN in longer time. Also the e-BN is likely to grow in low pressure in gas.

In conclusion, in nitrogen plasma, boron is more likely to react with nitrogen than in nitrogen gas. And h-BN, r-BN and e-BN have a preferred growth parameter of pressure.

Reference

1.Milton Ohring, Materials science of thin films, p130, Academic Press, New Jersey ,2006

2. Jun Sheng Li, Chang Rui Zhang, Bin Li. Applied Surface Science.257. 7752–7757.2011

3.Jos´e E. Nocua, Fabrice Piazza, Brad R.Weiner, and GerardoMorell. Journal of Nanomaterials, 2009, 429360, 1-6, 2009

4. A. Olszyna, J. Konwerska-Hrabowska, andM. Lisicki. Diamond and Related Materials. 6.p617–620, 1997.

Chapter 5 Conclusion

1. There is an energy density threshold existed for pulsed laser deposition of boron, and this threshold depends on the geometry of the system-especially if the direction of plume is upward or horizontal.

2. Particles ejected during pulsed laser deposition play an important role in film growth. It is difficult to avoid particles ejecting but to add filter or bias to decrease its number.

3. Surface morphology is also affected on the film deposition which results in unstable experiment data under same preparation conditions. Adding a rotating motor to control the rotation of target should help this situation.

4. The thickness of thin film is not uniform due to the distribution of plume. So to get more uniform thin film, substrate needs to be rotated and placed in the edge of plume.

5. Boron nitride prepared by reactive pulsed laser deposition makes it hard to characterize by XRD and Raman since its annealing temperature for crystallize is high. While, using FTIR can successfully get some boron nitride peaks. The peaks show some facts about different boron nitride phase preferred growth. In plasma enhanced PLD and nitrogen gas PLD, with pressure decreases, the amount of h-BN and r-BN phase will increases but amount of e-BN will decrease. Comparing to these two techniques, there is much more h-BN and r-BN prepared in former but much more e-BN in latter. After longer time for 30 minutes, the peak of h-BN disappears and e-BN becomes very strong. This means h-BN and r-BN can transform into e-BN after enough time.

VITA

Siwei Tang was born in Cili, Zhangjiajie city in Hunan province of China on March 18th,1984. He attends MingZu high school for studying from 1996-2002. Then he took the college entrance examination and enters Central South University for Bachelor's degree of "Technique of Measuring Control and Instrument" in department of Information from 2002-2006. Next he changed his major to "Materials science and engineering" then began two years of master student in department of Materials science and engineering in the same university. In 2008, he took an exam and is received as a Ph.D candidate in the department. He was married to Tian Tang before he attends University of Tennessee in August, 2009.